

**LNF-09/ 6 (IR)**  
**June 11, 2009**

**Conceptual Design Report**

**A PHOTO-NEUTRON FACILITY FOR TIME-OF-FLIGHT MEASUREMENTS**

Acronym: PNF

S. Bartalucci<sup>\*a</sup>, Vl. Angelov<sup>b</sup>, K. Drozdowicz<sup>c</sup>, D. Dworak<sup>c</sup>, G. Tracz<sup>c</sup>

<sup>a</sup>*INFN-Laboratori Nazionali di Frascati Via E. Fermi 40, I-00044 Frascati, Italy*

<sup>b</sup>*Institute for Nucl. Res. and Nucl. Energy, 72 Tzarigradsko chaussee blvd,  
1784 Sofia, Bulgaria*

<sup>c</sup>*The Henryk Niewodniczanski Institute of Nucl. Phys. – Polish Academy of Sciences  
ul. Radzikowskiego 152, 31-342 Kraków, Poland*

**Abstract**

The accelerator-based neutron sources, which are driven by electron Linacs, still appear quite attractive, notably because of their use in the cross section measurements with the time-of-flight method. This is due to their better beam quality and economy aspects, what make them complementary, and in some case even superior to the hadron (protons, deuterons) driven spallation facilities.

A conceptual design study of a powerful neutron source has been developed, aiming at the implementation on a future normal- or super-conducting Linac to be built in the Rome Research Area, but keeping enough flexibility for being installed on any high energy linac. The uniqueness of this source in Italy because of its white neutron spectrum and high TOF resolution has to be stressed. A general description of the facility is given in this report, with an illustration of the scientific case, of the main physical and technical issues that affect the source optimum design, and a tentative estimate of the costs and time scheduling required.

PACS.: 29.25.Dz; 01.52.+r

---

\* Sergio.Bartalucci@lnf.infn.it

## 1. Introduction

This project aims at the realization of a pulsed, high-intensity neutron source based upon an electron Linac for time-of-flight (TOF) measurements and other applications.

The distinguished features of this source that would make it unique among similar facilities are:

- optimized for primary electron beam at high energy, acting also as beam dump
- easy 'portability' , i.e. possibility of displacement from one accelerator to another thanks to the very effective radiation shielding
- simpler and smaller neutron producing target, hence better energy resolution
- non-parasitic operation of the source, as a final product of an otherwise used facility
- good flux at a given energy resolution, due to the very short flightpath.

The need for nuclear data, even in the low energy region ( $E_n \leq 10$  keV) is ever growing, as highlighted in the HIGH-PRIORITY REQUEST LIST (HPRL) of the NEA/OECD Data Bank [1]. Interaction of neutrons with matter is of great importance when evaluating the safety and risks related to operation of nuclear power plants, nuclear waste management, or new concepts of nuclear power production. Smaller uncertainties in the neutron cross-section data can result in enhanced safety of the present and future plants.

The technology of fission and fusion reactors, nuclear waste transmutation is the main application fields. Current programmes put much emphasis on data requirements for waste management (minor actinides and fission products), for new design of fission reactors including accelerator-driven systems (ADS), and for fusion reactor shielding, materials activation and heating studies.

Neutron interaction data in the energy range 0.001 eV to 20 MeV and the yield and decay properties of radioactive isotopes have been the data of primary interest for fission and fusion reactor studies. Data for the reactions induced by alpha and gamma radiation, and in particular for the neutron producing reactions alpha-n, gamma-n and gamma-f, are also needed but the accuracy requirements have not been so stringent.

Nuclear Astrophysics has acquired over the last 10 years an increasing interest for the scientific community. More accurate neutron capture data are needed, so that some facilities which were previously used for nuclear industry-related measurements, like Karlsruhe in Germany and ORELA in U.S., are now devoted to astrophysical studies.

Other relevant fields are found in synergies with ion beam analysis (mass spectrometry, non-destructive analysis) and with medical applications (e.g. radiotherapy, production of radioisotopes). The theory of nuclear structure, of fission process and the modelling of nuclear reactions are still looking for better data, while the possibility of fundamental physics investigations is also very appealing.

Present Linac-based TOF facilities are unable to satisfy all requirements, especially in terms of energy resolution, also because they're undergoing upgrading programmes, while the operating, starting, or planned high-power spallation sources are quite clearly not best suited to the TOF requirements.

Besides the HPRL, other databases of neutron-induced reaction cross sections are maintained by the Nuclear Energy Agency (NEA) of the Organisation for Economic Co-operation and Development (OECD), seated in Paris. In Western Europe the Joint Evaluated Fission and Fusion (JEFF) project of evaluated neutron data maintains a comprehensive database for routine applications in various areas of science and technology. Similar projects are present in Japan, with the JENDL Library maintained by the Japanese Atomic Energy Research Institute (JAERI), in the U.S. with the ENDF Data Bank and the National Nuclear Data Center (NNDC) in Brookhaven, partly supported by DOE, in Russia with the BROND library, coordinated at the Obninsk Inst. of Physics and Power Engineering and in China, where the Chinese Inst. of Atomic Energy coordinates the library CENDL.

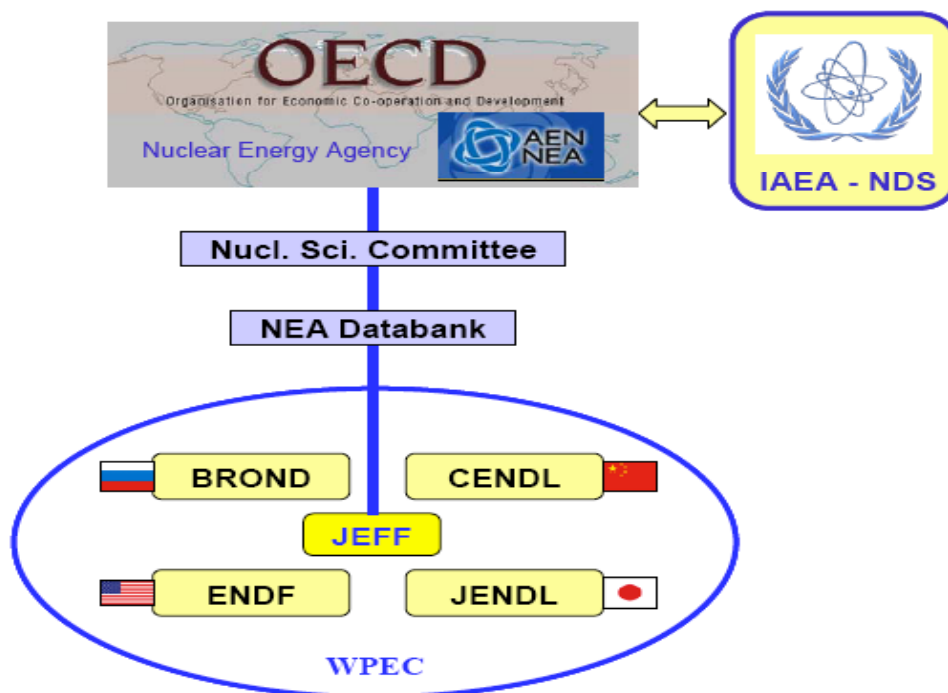


**Figure 1 The Nuclear Data Network**

The NEA Data Bank provides nuclear data services as part of the Nuclear Reaction Data Centres Network (NRDC). This is a worldwide co-operation of the aforementioned and other nuclear data centres, under the auspices of the International Atomic Energy Agency (IAEA) (see Fig. 1-2).

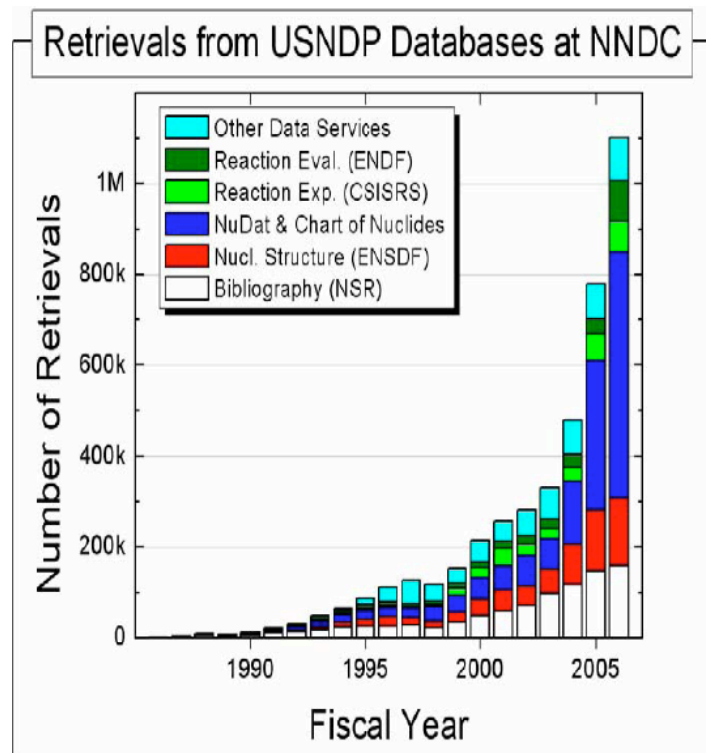


**Figure 2** The impressive ever-growing number of requests for nuclear data from various general- and special-purpose libraries maintained by NNDC

For accurate neutron data two energy domains need to be distinguished:

- \* the resolved resonance region, where the neutron cross-sections reveal a complicated resonance structure. Here, experiments with very high-energy resolution are required. This is only possible at dedicated time-of-flight facilities such as the linear electron accelerator (GELINA) facility at IRMM.
- \* the unresolved resonance region, where the width of the resonances is larger than the resonance spacing, and the overlapping cross-sections exhibit a smoothed energy dependence. In this energy region measurements with mono-energetic neutrons are preferable, which are usually obtained using nuclear reactions.

## **2. Needs for improved or new neutron data**

### **2.1 NEUTRON DATA FOR NUCLEAR POWER INDUSTRY**

Nuclear data are required for the design, safety assessment and operation of nuclear power plants and associated waste management facilities.

Neutron interaction data in the energy range 0.001 eV to 20 MeV and the yield and decay properties of radioactive isotopes have been the data of primary interest for fission reactor studies. Several types of data are needed, although not all with the same accuracy requirements: mostly cross-sections but also fission neutron spectra, prompt fission gamma spectra, fission fragments, delayed neutrons, covariance data, integral experiments.

The work involved in providing the neutron data required by the nuclear power industry can be separated into the following areas:

*Neutron standards* The majority of basic and applied measurements in neutron physics are performed relative to cross-section standards. These are given special consideration because of their importance in measurement and evaluation. Experimentalists to determine neutron fluence in cross-section measurements use standard neutron cross-sections; they are also particularly important for obtaining absolute fission cross-sections from fission ratio measurements. A consensus has arisen that certain of the neutron standard cross-sections need to be upgraded, and that a better understanding of the standards evaluation procedure is needed (particularly in relation to the magnitudes of uncertainties and covariance in the data).

It is therefore essential that these standards are continuously improved and their underlying physical mechanisms are understood.

The OECD and the Data Centre of the International Atomic Energy Agency (IAEA) have standards subcommittees to identify needs for new standards, for improvements of established standards and to regularly update the neutron standards data files. These standards data files are publicly accessible at no cost and are of major interest to various disciplines in science (physics, medicine, astrophysics) and technology. The detailed requirements for neutron data measurements, and in particular for improvements of the standards database, are collected in the HPRL of NEA.

For example, the  $^{10}\text{B}$  reaction cross section is amongst the most important standards used in neutron measurements. Over the years the EC Institute for Reference Materials and Measurements (IRMM), which operates the Electron Linac GELINA, has improved the data and this work has resulted in better branching ratio values solving the discrepancy observed for the  $^{10}\text{B}(n,\alpha)$  reaction during a standards evaluation [2].

*Measurements of “differential” or microscopic data* The word “differential” is used to distinguish basic data from “integral” or macroscopic measurements in which averages of the data are obtained. Integral measurements can be the average of reactions induced by neutrons having a range of energies or the average neutronics characteristics of a mixture of materials.

Differential measurements include measurements of cross-sections as a function of incident particle energy and the multiplicity, energy and angular distributions of secondary particles.

Some types of integral data can be measured on differential measurement facilities and the yields of products in fission are also basic measurements.

Typical differential measurements include:

- High-resolution total, capture and fission cross-sections in resonance regions. These require white

TOF facilities with white neutron spectrum.

- Energy and angular distributions of scattered neutrons or secondary particles
- Neutron- and charged particle-induced activation cross-sections.
- Yields of prompt and delayed neutrons in fissions.
- Yields of fission products and their decay properties
- Radioactive decay data of unstable nuclei

Differential data are openly published and are made generally available. For high-resolution cross-section measurements, from thermal energies to several MeV, pulsed white source time-of-flight facilities are needed. For all of these techniques, samples of the required elements or isotopes must be available and affordable. Differential measurements are still regarded as essential by evaluators and developers of nuclear theory.

The major western european facilities are presently carrying on an integrated project on data for nuclear waste transmutation within the Sixth Framework Programme (EFNUDAT) [3]. No italian facility is involved in this project, although italian group have performed measurements at some facilities within this project.

*Integral data measurements* These can be made on critical facilities or using specially tailored sources or benchmark fields. They are used to validate (and in some cases adjust) the differential data. When the form of the energy dependence of a cross-section is known, an integral measurement is sufficient for the normalisation of the cross-section. Such measurements can be closer to the parameters to be calculated and so provide a more accurate basis for their prediction. Integral measurements are often proprietary and only available to the organisations participating in the measurement programmes. Several facilities are available worldwide, mostly in Europe (CEA-Cadarache, Mol in Belgium, PSI in Switzerland, ENEA-Frascati and TU Dresden in Germany for fusion physics).

*Evaluation of the differential data* The task of the evaluator is to consider all of the relevant measurements and derive a recommended set of data. Nuclear theory can be used to interpolate and to help in making corrections to the measurements. Some data can be obtained just using theory when the accuracy requirements are not too stringent.

The present projects of Evaluated Nuclear Data Libraries have already been mentioned above. We must point out that several of these projects are suffering from insufficient resources being available to maintain the desired progress. The number of scientists engaged on evaluation and validation studies has declined significantly in some countries, with many retirements in the past 20 years. International cooperation has become more important as the number of scientists working in the field has declined.

*Validation of the evaluated differential data using the results obtained in integral measurements* Validation of evaluated data is an essential step before the data can be recommended for use and this activity requires an effort comparable to data evaluation, so this involves perhaps more than half of the total effort.

It is important to ensure that the integral database is appropriate for testing the accuracy of the data for the proposed applications. The nuclear data used in calculations can be adjusted to improve agreement with integral measurements. Unlike differential data, much of the integral data used for validation work is proprietary to the countries where the measurements were carried out or to the measurement-funding organisations. There is a danger of results being lost when a country discontinues its integral measurement programme or when staff retires, and both the NEA and IAEA NDS have initiated programmes to save integral data information. As an example, the SINBAD database, which contains the specifications for a number of shielding benchmarks relevant to fission reactors, fusion devices and accelerators, is maintained by NEA Data Bank and the RSICC (Radiation

Safety Information Computation Center) at Oak Ridge, USA.

*Processing nuclear data to the forms used in calculations* Energy group averaging of cross-section data is usual for routine calculations. Continuous energy Monte Carlo codes can represent the data more exactly, but there are still some approximations (the effect of Doppler broadening of resonances on secondary energy distributions, solid state effects, treatment of unresolved resonance regions, etc.) The NJOY code (developed at Los Alamos) [4] is widely used for processing evaluated interaction cross-sections.

*Assessing the accuracy of calculations* In principle, given the uncertainties in the differential data, and the sensitivity of calculated properties to changes in nuclear data, the accuracy of calculations can be estimated. However, the basic uncertainty information is far from complete and sensitivity calculations are not always easy to make. The uncertainty information is referred to as COVARIANCE DATA because the uncertainties in the values at different incident particle energies and for different types of interaction are correlated. The analysis of integral measurements can give a useful guide to the accuracy of predictions. In many cases it is easier to assess the accuracy of an integral measurement than the evaluated differential data.

## 2.2 NEUTRON DATA FOR NEW NUCLEAR CONCEPTS OR IMPLEMENTATION

*Partitioning and transmutation of nuclear waste* A satisfactory solution for the disposal of waste from nuclear power plants is a key issue for the future of nuclear energy production. The research in this field focuses on the partitioning (i.e. chemical separation) of long-lived radioactive isotopes in the nuclear waste and subsequent transmutation into short-lived or stable isotopes. Transmutation occurs via neutron capture or fission reactions by exposing the materials to high neutron fluxes. The goal is to burn the so-called long-lived fission products (LLFP) such as Tc-99, I-129, and Cs-135, and minor actinides (MA) such as Np, Am, and Cm isotopes.

There are three options for the reduction of long-lived radiotoxicity of nuclear waste:

1. using high fluxes of fast neutrons from a dedicated fast reactor or a spallation source using an accelerator driven system
2. recycling actinides and fission products in a molten salt reactor
3. using very high burn-up fuels in pressurised light-water reactors (PWR).

In all cases the knowledge of the associated nuclear data is not complete, and especially in case of the relevant reaction cross-sections in fast reactor systems and accelerator-driven systems.

Total and capture cross-sections on Tc-99 and I-129 have been measured with high-energy resolution at IRMM. [5]. Several reaction cross sections for these isotopes were also determined with the activation technique and total and capture cross-section measurements on Np-237 have been carried out. Measuring Am-241 is planned.

*Neutron data for accelerator driven systems* Different types of "dedicated waste transmuters", either critical or subcritical, like the accelerator driven systems (ADS) for transmutation of nuclear waste, have been proposed and are currently under investigation [6].

A very promising one is based on a liquid Pb-Bi spallation target (the MYRRHA concept)[7]. The main components to be investigated are the spallation target, the target-core interface, the core, moderator and coolant, the support structure and shielding.

Characteristic for this system is that the target and the target-core interface, the core and the support structures close to the target are subjected to neutrons of high energies. Energies up to several GeV are possible, the highest energies hitting the target and target support area. Just outside the target

area the neutron energies range up to a few tens of MeV, whereas at larger distances from the target the neutron spectrum approaches that of a conventional fast (or thermal) reactor.

Some EC programmes, such as EUROTRANS/NUDATRA and n\_TOF-ND-ADS, fund nuclear data work for Accelerator Driven Systems (mainly on Pb, Bi for the MYRRHA concept) [8].

For a complex system like an ADS, many cross-sections and reaction parameters are important. The total, capture, elastic and inelastic scattering, and fission cross sections as well as light charged particle production cross-sections (e.g. for hydrogen and helium emission) relevant for damage of structural materials are also of relevance to an ADS.

As an example, the potential impact of nuclear data uncertainties on a large number of performance parameters of an ADS is described in [9].

An uncertainty study was performed based on sensitivity analyses, which did underline the cross sections, the energy range, and the isotopes that were responsible for the most significant uncertainties. The integral parameters analyzed in [10] were all the ADS parameters potentially most sensitive to nuclear data uncertainties: multiplication factor, power peak, defined as the point maximum power value normalized to the total power, burnup  $\Delta k/k$ , coolant void reactivity coefficient, nuclide density at end of cycle (transmutation potential), the ratio  $\phi^*$  of the average external source importance to the average fission neutron importance, the values of the displacements per atom (dpa), He production, H production and the ratio (He production)/dpa at the spatial point where they reach their maximum value (Max dpa, Max (n, $\alpha$ ), Max (n,p), Max (n, $\alpha$ )/dpa) (See Table I-a and -b).

An assessment of target accuracy requirements was performed for an ADS system which has some general features (e.g., the mass ratio between plutonium and MA, the americium-to-curium ratio, etc.) that are representative of the class of MA transmuters with a fast neutron spectrum and a uranium-free fuel. As a result, it can be observed that tight requirements are found for MA (minor actinides) cross-sections, in particular for  $\sigma_{\text{fiss}}$  of Cm-244, Am-241, Cm-245, Am-243, Cm-242, Am-242m, for  $\sigma_{\text{inel}}$  of Am-243 and for  $\nu$  of Cm-244. For these reactions, the required accuracies are an order of magnitude below the present uncertainties.

Concerning the major actinides, improvements are required for  $\sigma_{\text{fiss}}$  of Pu-241 (again  $\sim$  factor 10), for  $\sigma_{\text{fiss}}$  of Pu-238 ( $\sim$ factor 5) and for  $\nu$  of Pu-238 ( $\sim$ factor 3). Finally, important requirements are also found for structural materials, particularly for  $\sigma_{\text{inel}}$  of Fe-56, Bi-209, Pb and Zr-90.

Isotope	Cross-Section	Energy Range	Uncert. (%)		Isotope	Cross-Section	Energy Range	Uncert. (%)	
			Initial	Target				Initial	Target
Cm244	$\sigma_{fiss}$	6.07 - 2.23 MeV	31.3	3.0	Bi209	$\sigma_{inel}$	2.23 - 1.35 MeV	34.1	2.8
		2.23 - 1.35 MeV	43.8	2.6			1.35 - 0.498 MeV	41.8	4.2
		1.35 - 0.498 MeV	50.0	1.5	Am243	$\sigma_{fiss}$	6.07 - 2.23 MeV	11.0	2.3
Fe56	$\sigma_{inel}$	6.07 - 2.23 MeV	7.2	2.5			1.35 - 0.498 MeV	9.2	1.6
		2.23 - 1.35 MeV	25.4	1.6	Cm244	$\nu$	6.07 - 2.23 MeV	11.1	2.5
		1.35 - 0.498 MeV	16.1	1.5			1.35 - 0.498 MeV	5.5	1.3
Am243	$\sigma_{inel}$	1.35 - 0.498 MeV	42.2	2.3	N15	$\sigma_{el}$	1.35 - 0.498 MeV	5.0	1.2
		498 - 183 keV	41.0	3.6	Pb	$\sigma_{inel}$	6.07 - 2.23 MeV	5.4	2.9
		183 - 67.4 keV	79.5	3.7	Zr90	$\sigma_{inel}$	6.07 - 2.23 MeV	18.0	3.3
Pu241	$\sigma_{fiss}$	1.35 - 0.498 MeV	16.6	2.1	Pu238	$\sigma_{fiss}$	2.23 - 1.35 MeV	33.8	6.0
		498 - 183 keV	13.5	1.7			1.35 - 0.498 MeV	17.1	3.4
		183 - 67.4 keV	19.9	1.7			498 - 183 keV	17.1	3.9
Am241	$\sigma_{fiss}$	6.07 - 2.23 MeV	11.7	1.7	Cm242	$\sigma_{fiss}$	6.07 - 2.23 MeV	52.6	26
		2.23 - 1.35 MeV	9.8	1.4			498 - 183 keV	66.0	28.4
		1.35 - 0.498 MeV	8.3	1.2	Pu238	$\nu$	1.35 - 0.498 MeV	7.0	2.8
Cm245	$\sigma_{fiss}$	1.35 - 0.498 MeV	49.4	3.3			498 - 183 keV	7.0	3.4
		498 - 183 keV	37.2	2.9	Am242m	$\sigma_{fiss}$	498 - 183 keV	16.6	4.8
		183 - 67.4 keV	47.5	2.9			183 - 67.4 keV	16.6	4.8
		67.4 - 24.8 keV	26.5	3.2					

**Table I-a Uncertainty reduction requirements to meet integral parameter target accuracies [10]**

Table I-b shows the initial integral parameter uncertainties and the calculated uncertainties with the required cross-section uncertainties, as obtained with the minimization procedure.

	$k_{eff}$ [pcm]	Power Peak	Void	Burnup [pcm]	$\phi^*$	Max dpa	Max (n, $\alpha$ )	Max (n,p)	Max (n, $\alpha$ )/ dpa
<b>Initial</b>	1882	14.2	13.1	603	1.43	20.53	9.71	16.29	13.12
<b>With required uncertainties</b>	283	2.2	3.5	216	0.34	3.18	5.29	3.47	5.16

**Table I-b Integral parameter uncertainties(%)with initial and required  $\sigma$  uncertainties [10]**

*Neutron data for IV generation reactors* The next generation of nuclear energy systems - generation IV - must be licensed, constructed and operated in a manner that will provide a competitively priced supply of energy. Challenging technology goals are defined in 4 areas: sustainability, economics, safety and reliability, and proliferation resistance and physical protection.

Recognizing both the positive attributes and shortcomings of the prior generations of reactor designs, 10 countries (among which Euratom is considered as a country) are working together to lay the groundwork for a fourth generation, called Generation IV. The governmental entities are working together as the Generation IV International Forum (GIF).

Because the next generation of nuclear energy systems will address needed areas of improvement and offer great potential, many countries share a common interest in advanced research and development. Such development will benefit from the identification and promising research areas and collaborative efforts that should be explored by the international research committee.

Six types of design are considered to be of "Generation IV" (see Table II [11]):

System	Neutron spectrum	Coolant	Temp. °C	Fuel cycle	Size (MWe)
VHTR (Very-High-Temperature Reactor)	thermal	helium	900-1 000	open	250-300
SFR (Sodium-cooled Fast Reactor)	fast	sodium	550	closed	30-150 300-1 500 1 000-2 000
SCWR (Super-Critical Water-cooled Reactor)	thermal/ fast	water	510-625	Open/ closed	300-700 1 000-1 500
GFR (Gas-cooled Fast Reactor)	fast	helium	850	closed	1 200
LFR (Lead-cooled Fast Reactor)	fast	lead	480-800	closed	20-180 300-1 200 600-1 000
MSR (Molten Salt Reactor)	fast/ thermal	fluoride salts	700-800	closed	1 000

**Table II The Generation IV reactors**

The status of relevant nuclear data for the Gen-IV reactor development is subdivided in the 4 categories of minor actinides, moderator, burnable poison and fission products nuclides.

For fast reactors (GFR, LFR, SFR and SCWR for actinide recycle), the main data needs are cross sections in resolved resonance region and above, owing to incomplete knowledge:  $(n,n')$ ,  $(n,2n)$ , fission yields,  $n$  multiplicities, delayed  $n$ , light charged particle (LCP) emission ( $n,\alpha$ ;  $n,p$ ; ...).

New evaluations for fission products, which include full covariance information, are required to respond to the need for more stringent safety margins; to the tendency to operate present power plants (GEN III and GEN III+) at increased fuel burnup; and for criticality safety of spent fuel transport and storage. Improved capture and total cross-sections for several fission products (i.e.  $^{103}\text{Rh}$ ,  $^{133}\text{Cs}$ ,  $^{143}\text{Nd}$ ,  $^{149}\text{Sm}$ ,  $^{151}\text{Sm}$ ,  $^{155}\text{Gd}$  and  $^{131}\text{Xe}$ ) are on the HPRL.

Other crucial issues are resonance shapes (Doppler broadening, poisons) and delayed neutrons.

Since most Gen-IV reactor concepts employ very long fuel reload cycle to increase the economics goal, the accuracy of slowly burning poison is stressed than before. The current status of a typical slowly burning poison, Europium[12], is shown in Fig. 3. The discrepancy between existing libraries is impressive.

In the MSR, where the nuclear fuel is dissolved in the molten fluoride salt coolant as uranium tetrafluoride ( $\text{UF}_4$ ), the use of the Thorium fuel cycle (with reprocessing), so impractical in other types of reactors, produces 0.1% of the long-term high-level radioactive waste of a light-water reactor without reprocessing (all modern reactors in the U.S.). But much more accurate data are required about the U-Th cycle and the Actinide recycle.

The VHTR is a helium-gas-cooled, graphite-moderated, thermal neutron spectrum reactor with a core

outlet temperature higher than 900°C, and a goal of 1000°C, sufficient to support high temperature processes such as production of hydrogen by thermo-chemical processes.

Several parameters are poorly known at high temperatures: criticality safety, transients, (n,n'), (n,n'γ), (n,2n) cross-sections (also important for ADS), accurate resonance integrals, fission cross-sections, parameters  $\alpha = \sigma_c/\sigma_f$  and  $\eta = \nu \sigma_f/\sigma_t$  ( $^{239}\text{Pu}$  !), fission yields, kinetic energy distributions, n multiplicities, delayed n, tritium production via ternary fission, light charged-particle production cross-sections, accurate temperature-dependent resonance shapes etc.

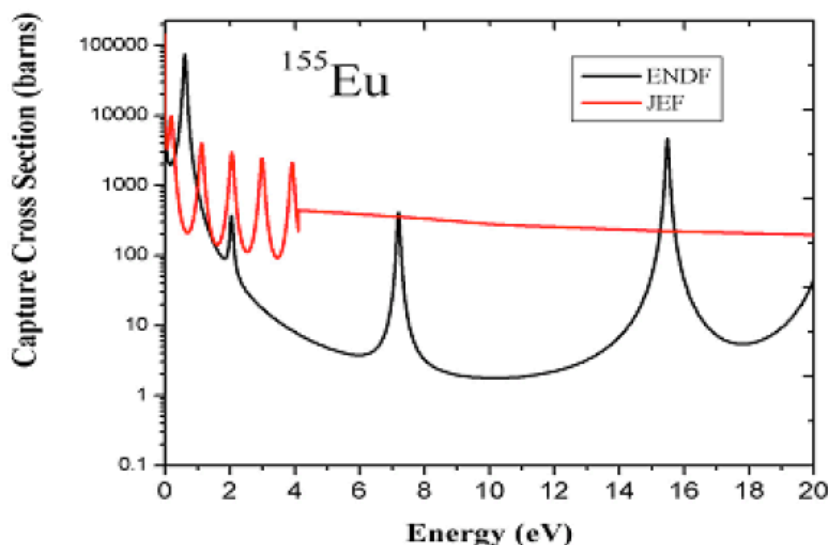


**Figure 3 Discrepancy between actual data libraries for the neutron capture  $\sigma$  of Eu [12]**

*Neutron data for fusion reactors* Fusion research worldwide is focused on developing the ability to generate electricity. The main areas of work are in support of the ITER and IFMIF project; ITER is a large experimental device that will be constructed at Cadarache in France while IFMIF is a material testing facility. Following the successful outcome of these projects it will be possible to design and build DEMO which will generate electricity and act as a prototype for future commercial designs. Nuclear data for fusion can be broadly split into three parts: cross sections for neutronics, cross sections for activation and decay data. Activation calculations require cross sections for a larger number of target nuclides than transport since both stable and radioactive targets must be considered. The reason is that in high neutron fluxes long-lived radioactive nuclides are present long enough to react, leading to multi-step pathway production of activity. However, although about twice as many targets and many more reaction types are needed than in a transport file, only cross sections as a function of energy data need to be included. Another type of nuclear data that must be considered, especially for activation calculations, are decay data including half-lives, energy releases and decay modes.

Activation impurities in fact dominate the response in terms of activity or gamma dose rate. This means that once data libraries have been assembled it is necessary to determine which radionuclides are important and the reactions that are responsible for their production. The current data library for activation used extensively in European Studies is EAF-2007. Not all of these data are of equal weight for fusion application, and it is crucial that they are ranked so that scarce resources can be concentrated on the most important. The main tool for this are importance diagrams [13] and an

example of determination of the important radionuclides and reactions is shown in Fig. 4 for Vanadium. The diagram is generated following a series of inventory calculations carried out with mono-energetic neutrons, and the nuclides that dominate, i.e. produce more than 50% of the dose at various decay times are identified. These results are then shown in the diagram by regions labelled by the nuclide. Thus at decay times greater than  $\sim 1 \cdot 10^7$  s at energies  $< 5$  eV and  $\sim 100$  eV there are two regions where  $^{60}\text{Co}$  dominates. Below 20 MeV this diagram is similar to that shown in the ‘Activation Handbook’ a large compilation containing importance diagrams covering the energy range up to 20 MeV for all the elements, calculated with EASY-2007[14]. Minor differences are due to changes in the cross sections between the two libraries. Of more interest is the new region above 20 MeV where three new nuclides are shown:  $^{48}\text{V}$ ,  $^{44}\text{Sc}$  and  $^{40}\text{K}$ .

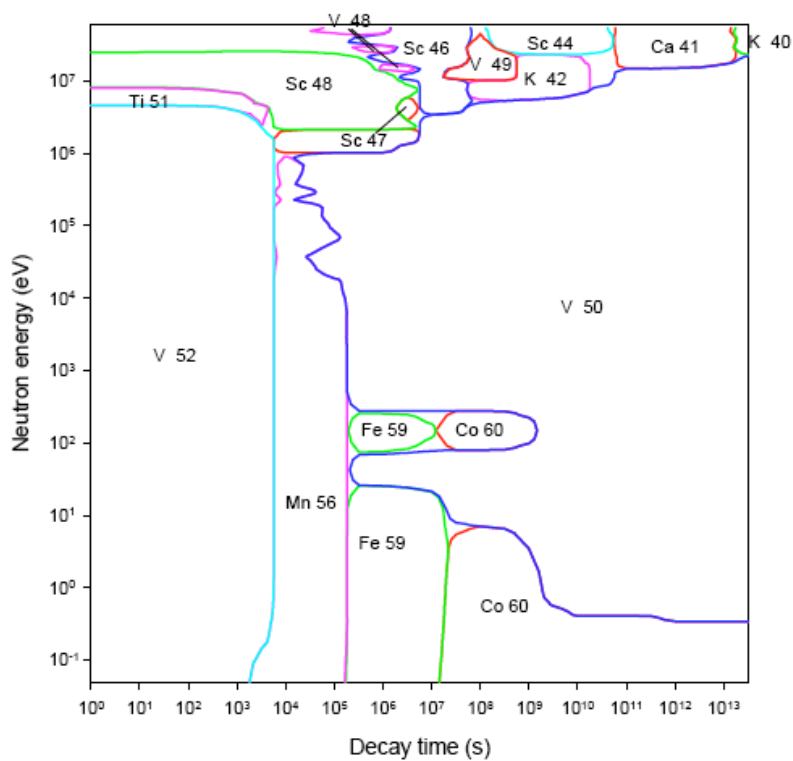


**Figure 4 The importance diagram for Vanadium [14]**

## 2.3 NEUTRON DATA FOR ASTROPHYSICS AND BIOMEDICAL APPLICATIONS

*Astrophysics* Nuclear astrophysics is another field where neutron data are essential for the understanding of the production of heavy elements in the Universe, which occurs mainly through slow and rapid neutron capture processes, during the various phases of stellar evolution.

These measurements are used to determine the rates of nuclear reactions needed to test and improve models of the big bang, stars, supernovae, and the chemical evolution of the galaxy as well as to obtain improved estimates of the age of the universe. Recent advances in astronomical observations, improvements and changes in astrophysical models (driven by ever faster and larger computers), and new nuclear physics measurement techniques have resulted in the need for more, new, and improved cross-section measurements. For example, recently it has been shown that making  $(n,\alpha)$  measurements on intermediate-weight nuclides could be perhaps the best method for improving the rates of  $(\gamma,\alpha)$  reactions needed for explosive nucleosynthesis calculations [15]. The rates for these reactions are very difficult or impossible to determine directly using current

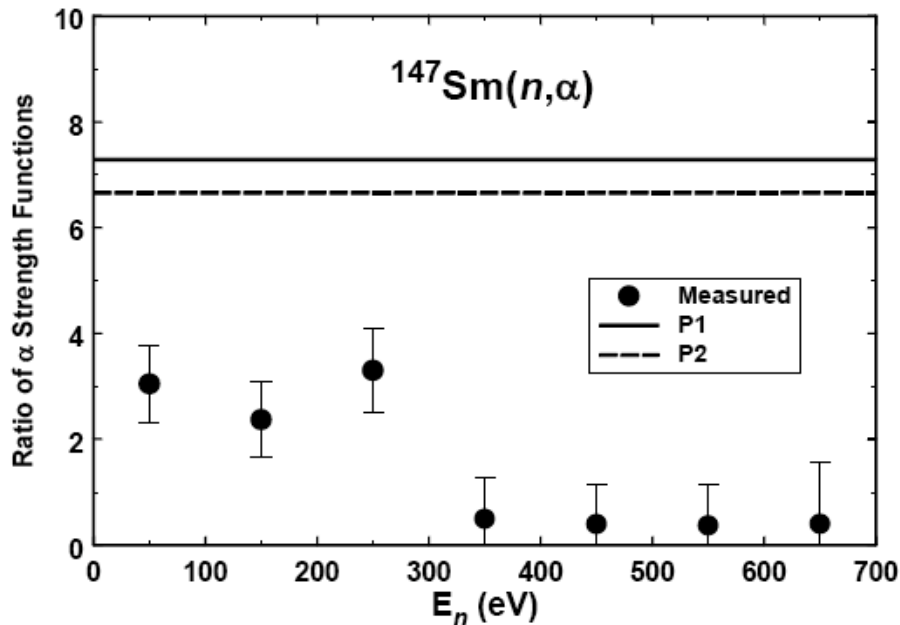


**Figure 5** Ratio of  $\alpha$  strength functions for 3 to 4 resonances populated in the  $^{147}\text{Sm}(n,\alpha)$  reaction [15]. The circles with onestandard-deviation error bars were obtained from a resonance analysis of cross-section measurements at ORELA. The two curves labeled “P1” and “P2” show the expected ratios calculated using the nuclear statistical model with two different input  $\alpha$ -nucleus potentials.

techniques, and the nuclear model used to calculate these rates is not very well constrained and hence has been unreliable. The first  $(n,\alpha)$  measurements in the energy region 100-700 eV have demonstrated that they should be very useful for improving the nuclear model, but have turned up some surprises [Fig. 5]. More measurements of this type are needed to improve the accuracy of  $(\gamma,\alpha)$  rates across the wide range of masses needed by the astrophysical model.

A considerable growth in this field is being testified by the availability of incredible images and data from powerful space- and ground-based observatories (e.g., Hubble, Chandra, Wilkinson, Keck,

Subaru, and others), as well as the sophisticated astrophysical simulation codes that run on the fastest supercomputers. With new nuclear accelerator laboratories on the horizon (e.g., RIKEN RI Beam Factory, GSI/FAIR, RIA) that promise a big amount of new data, this growth will definitely continue in the future.

Improved nuclear science is needed, for example, to decipher the latest measurements using satellite observatories of long-lived radionuclides (e.g.,  $^{26}\text{Al}$ ,  $^{44}\text{Ti}$ ,  $^{18}\text{F}$ ) that are synthesized in and dispersed by supernova and/or nova explosions. Improved nuclear data – especially uncertainty and covariance information – is also needed for studies that attempt to *quantify* what portion of the uncertainties in astrophysical predictions (e.g., for X-ray bursts) is due to uncertainties in the input nuclear physics. New multidimensional astrophysics supercomputer simulations (e.g., for supernovae) require more, and more precise, nuclear data, than ever before. Finally, a combination of astrophysical

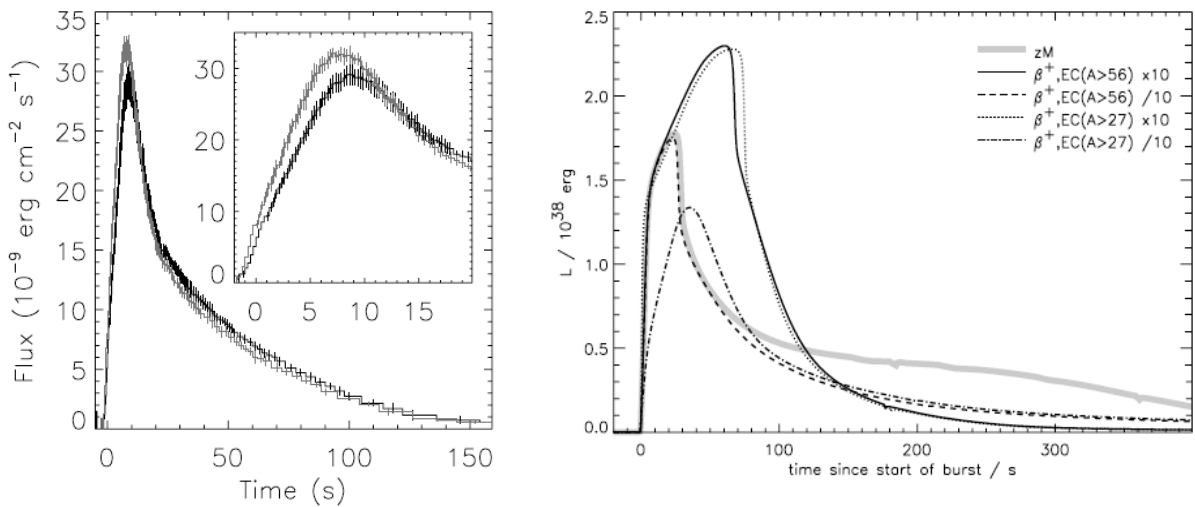


**Figure 6** The variation of X-ray flux in time from X-ray burst RXTE GS1826-24 [16], left, compared to the predictions of theory [17] using different input nuclear data sets, right.

observations, astrophysical simulations, and nuclear datasets are being synergistically fused in a new

generation of studies of the sensitivity of model predictions on input nuclear data (e.g., fig. 6) – and improved nuclear datasets will tremendously aid this work.

*Neutron Radiotherapy and Microdosimetry* The use of neutron beams in cancer radiotherapy was proposed soon after the neutron discovery by Chadwick in 1932 and experimented already in 1939 by Stone [18]. In particular, the radiotherapeutic technique named BNCT (Boron Neutron Capture Therapy), which was applied for the first time by Sweet [19] by the end of 40's after a long period of ups and downs, is nowadays earning a renewed interest worldwide and also in Italy, especially from the nuclear research institutes, like ENEA and INFN and from some Universities and Hospital Institutions.

The therapeutic benefit of BNCT is due to the passage of highly ionizing particles, as produced in the reaction  $^{10}\text{B}(n, \alpha)^7\text{Li}$  which occurs with an energy release  $Q = 2.792$  MeV and is induced by thermal neutrons ( $E < 0.4$  eV). (see fig. 7)

The  $\gamma$  emitted after neutron capture in  $^{10}\text{B}$  is not very useful for therapy purpose, but it could be helpful as a marker of the just occurred reaction, while the two other particles ( $\alpha$  and  $^7\text{Li}$  nucleus) lose all their energy inside the traversed cell (within a mean range of  $8 \mu\text{m}$ ), by leaving a very dense

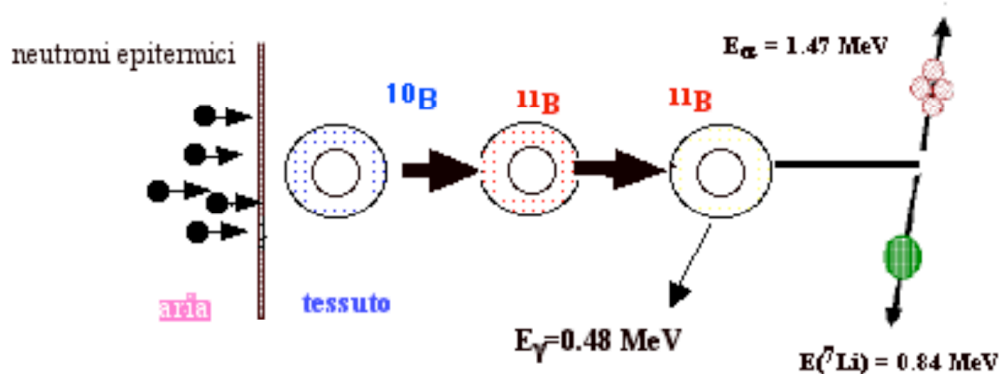


Figure 7 The BNCT mechanism

ionization wake. The resulting electric field is able of segmenting the 2 DNA helices at the same quotation, thereby inactivating the cell with high probability.

The motivations for the  $^{10}\text{B}$  choice are not only the high thermal neutron capture cross section, but also and mostly its chemical properties, like its high capability of forming stable chemical compounds with Carbon, Oxygen and Nitrogen. Other nuclides have similar nuclear properties, like  $^6\text{Li}$ ,  $^{157}\text{Gd}$ , even  $^{235}\text{U}$ , but are not as good from the biochemical point of view, although research has not progressed much in this field from the years 50's. The effectivity of the therapy is linked to the B concentration in cytoplasm of malignant cells, which should be at least a factor 2 (4 in the liver tumour) higher as compared to the concentration in the normal cells. The maximum allowed radiation dose is still limited by the tolerance of the nearby normal tissue, and unfortunately the selective destruction of cancer cells remains a non-achieved goal. BNCT was used in the past for several clinical applications, starting from multiform glio-blastoma (GBM) and cutaneous melanoma, to multifocal liver tumours, as treated with explantation, external irradiation and re-implantation of the organ, up to the intra-operation post-surgical treatment (IORT) with hospital Linear Accelerators. Major achievements in this sector would drive research towards application to other types of cancer, such as small lung cell carcinoma, neck and head tumours, osteosarcoma etc.

In all the above cases the targeted organs are *directly* exposed to thermal neutron beams, but this condition is not always fulfilled, e.g. if the tumour is deeply seated in the body or the patient is not operable without serious clinical complications.

Research was oriented in the past towards three main goals:

- [1] Design, synthesis and evaluation of more selective tumour targeting agents
- [2] Optimizing their delivery
- [3] Improving neutron beam characteristics from reactors and accelerators

On this last item it may be observed that remarkable difficulties were found in the realization of neutron beams of energy suited to the treatment of deeply seated and inoperable cancers (epithermal beams,  $0.4 \text{ eV} < E < 10 \text{ keV}$ , with a few cm penetration power in soft tissues). *White spectrum* neutron beams (as from excitation and evaporation of heavy nuclei) have already been used indeed in several places in the world, though with uncertain results.

The possibility of using medical electron Linacs, which are available in several hospital institutes for the IORT technique, in combination with Be target to produce neutrons for BNCT, is now currently investigated within INFN, but it doesn't seem able to overcome the power limits of such machines without introducing additional risks and difficulties.

More recently, the use of *energetic* neutron beams (0.1 - 10 MeV), in combination with BNCT, allowed the re-discovery of another technique, named BNCEFNT (Boron Neutron Capture Enhanced Fast Neutron Therapy) [20], which has already been proposed at the end of 70's years, and is now currently investigated at several radiotherapy centers worldwide, such as the Washington University (UW), the FNT facility of Harper's Hospital in Detroit (Michigan), the Neutron Therapy facility (NTF) of Fermilab (Illinois), the National Accelerator Centre (iThemba, South Afrika) and the Biomedical Cyclotron of Nice, France. Indeed, the integration between the FNT technique, which has already proven successful in some non-cerebral tumours (such as salivary gland tumours, advanced phase prostate cancer, unoperable cancer of non-small cell lung cells, soft tissue sarcoma and osteosarcoma), and the BNCT may reveal useful in the treatment of radioresistant brain tumours, like the multiforme glioblastoma. In some cases, the use of  $^{10}\text{B}$  enriched targets (tissue-equivalent ionization chambers) with various neutron filters allowed a percentual dose enhancement (PDE) of 10-15% (measured) and up to 30% in case of simulations with mathematical models of human phantoms, keeping nevertheless a high level of total absorbed dose, as sufficient to therapy treatment. Nobody has been treated in BNCEFNT till now.

The usual neutron sources, such as nuclear reactors, D-D fusion generators and hospital Linacs, which are mostly envisaged for use in BNCT, are not suited for a detailed study, owing to experimental difficulties in the beam preparation and characterization in interesting energy regions. High energy linac - based neutron sources are instead unapted to therapy practice, but seem definitely superior for the high energy resolution achievable, thereby allowing for a detailed study of the relevant fundamental processes, aiming at a dramatic improvement in the neutron dose assessment and in the beam quality optimization for radiotherapy. In fact, if we know pretty well the biological effects of various charged particles which are generated by neutron interactions with the most common nuclei which are present in the human tissues, the cross sections (double differential) for the production of those particles are much less known. A deeper knowledge of those processes would certainly allow for a better understanding of some still unexplained facts, such as, e.g., the remarkable difference (even by an order of magnitude) in the cell survival time if the same dose is imparted with neutron,  $\gamma$  or electron beams. This difference is generally ascribed to the different ionization densities, which affect the cell damage and self - repair. One should consider that present dosimetric methods and treatment techniques are indeed based upon integral quantities (kerma coefficients) and experience, rather than on a thorough analysis of fundamental physics.

All in all, it seems quite evident that BNCT can progress significantly only by a combined effort from the development of new neutron sources, which are able to deliver beams suited to the tumour specificity, an even more accurate data acquisition about elementary reactions which are induced by neutron passage in matter (Microdosimetry), and a deeper understanding of biochemical and physiological requirements for tumour targeting.

The research programme that can be implemented on a Linac-based neutron facility is then described as follows:

- 1) Development of a microdosimetric model for better understanding of BNCT effects on a cell scale. The model (of the MICOR kind [21]) should be able to allow computing of fractional cell survival, RBE (Relative Biological Effectiveness) values and Boron concentration distributions.
- 2) Study of a mathematical anthropomorphic phantom (e.g. 'ADAM' [22]) to be implemented on the well-known codes FLUKA e MCNP.
- 3) Detailed study of other nuclear reactions which enable dose absorption (e.g.  $^{35}\text{Cl}(n,g)^{36}\text{Cl}$ ,  $^{14}\text{N}(n,p)^{14}\text{C}$  etc.) in the main elements which are present in human tissues, such as carbon, oxygen, nitrogen, chlorine e calcium.
- 4) Study of neutron field with proportional counters, GEM (Gaseous Electron Multiplier) and tissue-equivalent silicon detectors. Microdosimetric calculations of the effective biological dose and comparison with experimental results.

- 5) Study of new Boron Compounds with biochemical and physical-chemical properties such that the tumour targeting can be produced *in vivo* and optimization of their delivery to the clinical level. In particular, organic polymers which may be more suited to specific interaction with tumours, the selection of proteical vectors which are tumour-specific and of more efficient nuclear targets and the preparation of complex bio-substrate which are necessary for irradiation tests.
- 6) Study of possible use of other chemical elements with high neutron absorption (like Gd) in addition/alternative to Boron as far points 1) e 5) are concerned.

## 2.4 NEUTRON DATA FOR NUCLEAR THEORY

*Nuclear structure* The study of neutron resonances has been at the center of nuclear physics since the very early days. The discovery of sharp quasi-stationary states in the highly excited nuclear system led Bohr to formulate his compound nuclear hypothesis. In the late 1940s and throughout the 1950s, there was an explosion of measurements of neutron cross sections. Various reaction models were developed; almost all were of a statistical nature and in slightly different form remain in use today. Phenomenological level density models were developed; most followed the Bethe ansatz, and used some variation of the original Fermi gas model. Again these approaches are still very much in use today. Individual resonances and their energy, widths, and quantum numbers were characterized by the use of the Wigner-Eisenbud formalism as summarized by Lane and Thomas [23]. However, the overall description of the set of resonances raised serious questions. Since for heavy nuclei the wave functions for the individual resonances have 10<sup>5</sup> or more components, the only possible description is statistical.

Wigner proposed the use of random matrices to describe the level statistics and the width distributions. Dyson extended the theory and proposed a number of useful measures. The predicted statistical properties of the spectra are usually called Wigner-Dyson statistics. Standard measures include the Wigner surmise (the expression for the nearest-neighbor spacing distribution (NNSD) that shows the famous level repulsion), the Dyson-Mehta  $\Delta_3$  statistic that measures the long range order, and the Porter-Thomas distribution for the reduced widths that is characterized by a very large number of small widths.

Although the theory was well formulated by 1963, there were no data of sufficient purity and completeness to test the theory for a long time. In 1983 Bohigas combined the best available resonance data and demonstrated that the data agreed well with the expected Gaussian Orthogonal Ensemble (GOE) version of Random Matrix Theory (RMT)[24]. About this time Bohigas also made his famous conjecture that connected the character of the level statistics (Poisson or GOE) with the degree of chaoticity (regular or chaotic). Applications of RMT have since expanded exponentially, in fields as diverse as quantum dots and lattice gauge calculations. However, there has been relatively little progress in nuclear physics due to the stringent requirements on the data. The original evaluation of the best resonance data is now over 20 years old. The only other large scale evaluation was of low-lying states and is now nearly 15 years old. These studies should be redone and additional measurements are in order. It has been suggested that these compilations be reexamined and that some of the key heavy nuclei be remeasured.

The newer and older neutron facilities should provide important information for the exciting area of chaos and complexity in nuclei.

*The fission process* Fission has been and still remains a central problem for physicists involved in nuclear energy production. Still, despite the seniority of the enterprise, the present description of the fission process remains largely dominated by phenomenology. In the last years of the sixties, the Nilsson-Strutinsky model provided an opening by allowing a semi-microscopic calculation of fission

barriers. Few years later, advances in the definition of density functionals led to the first fully microscopic calculations (HF+BCS and HFB methods) of the fission barrier of  $^{240}\text{Pu}$  taking into account in a coherent manner, both the mean-field and the pairing component of the nucleon-nucleon effective interaction. Until recently, further progress has been rather slow. In fact, what was needed was a density functional theory with a predictive capacity of a global nature (the full chart of isotopes, a large set of ground state and excited state properties). This long investigation if not concluded yet, seems at least to have reached a more satisfactory state. Microscopic theory is now in the position to predict masses and fission barriers with an accuracy as good as that of the most accurate phenomenologies [25]. In addition, the greatly enhanced computing power gives the possibility of fast and systematic calculations of fissionfusion energy surfaces as a function of

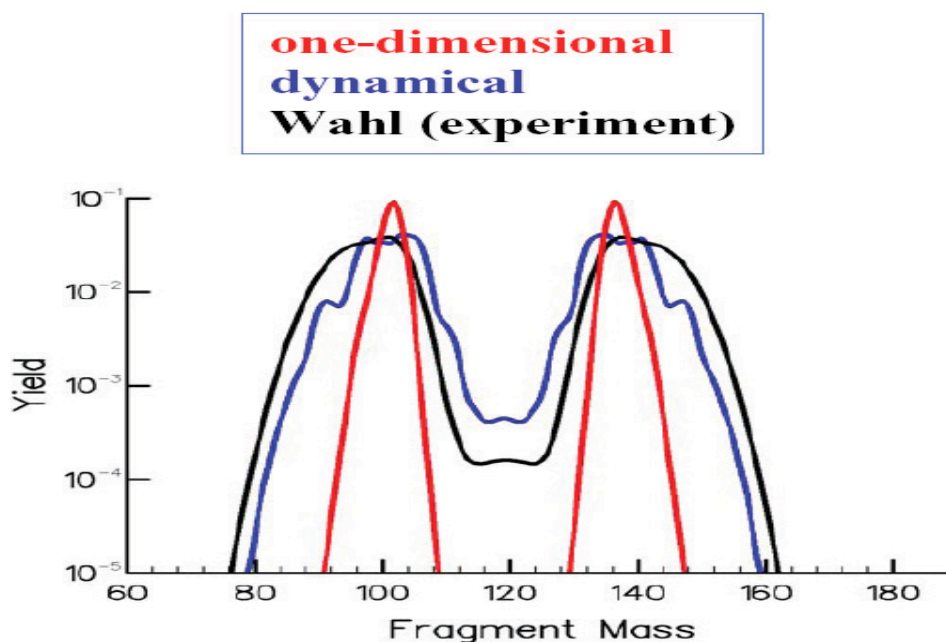


**Figure 8** Distribution of fission fragments of  $^{238}\text{U}$ . The red solid line corresponds to a one-dimensional dynamics along the fission valley bottom while the blue curve takes into account the full energy surface.

multipole variables which take into account the complete set of shapes that a nucleus go through on its way to fission. As exciting such results may be, they still only correspond to half the solution. It is not enough to describe the static landscape over which fission takes place. One must also give a quantum description of the dynamics. It is only recently that encouraging results have been published [26]. Figure 8 is one such example. It shows the distribution of fission products of  $^{238}\text{U}$ . Similar encouraging results have been obtained for fragment kinetic energies and half-lives.

Thus, when experiment is out of reach, it seems now that exclusive reliance on phenomenology for prediction may not last. However, there is still more work ahead. There are several approximations in the method of solution of dynamical equations. Success must be confirmed on a much more extended set of nuclei. Finally, there remains to build a full N-body theory of the fission process. Such a theory would avoid the recourse to collective variables. Indeed, however plausible their choice may be, they are still an ad-hoc physicist's input into the microscopic description. Fission is the paradigm of the nuclear-large-amplitude-collective-motion. Any advance towards its solution will impact every aspect of that important subfield of nuclear structure for which collective motion is relevant.

*Nuclear reaction models* Continuous-energy (“white”) neutron sources have been used since the 1950s to measure the resonant structure in the energy dependence of neutron cross sections across the periodic table. In many applications the properties of these resonances (position, partial widths, total width) are used directly. In others, energy averages over the resonant structure are the important quantities; these energy averages determine the low-energy behavior of the nuclear optical model, which is a key ingredient in nearly all descriptions of nuclear reactions, including statistical models (e.g., Hauser-Feshbach) and distorted-wave Born approximation (DWBA) direct-interaction models. The measured average spacing of the *s*-wave resonances provides a critical check on the level densities used in statistical reaction models. Since properties of individual resonances can be measured only over a limited energy range, a typical problem is how to determine the energy interval over which the energy-averaged resonance parameters applies. This question addresses the issue of intermediate structure, which can invalidate the conventionally used forms of reaction models, such as the optical model and radiative capture. The importance of intermediate structure can only be answered if the experimental data base is sound, and this is where newer and older TOF facilities can make significant contributions (see fig. 9).

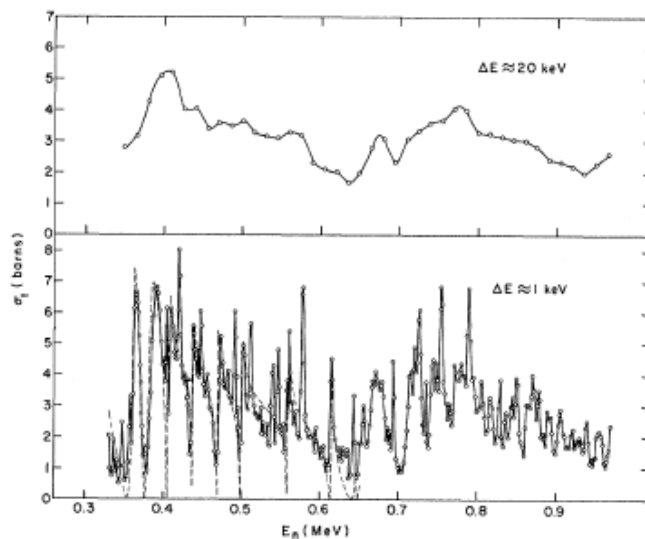


**Figure 9** The intermediate structure in the total neutron cross section of  $^{56}\text{Fe}$  which shows evidence for structure with widths on the order of 100 to 200 keV [27]

## 2.5 FUNDAMENTAL PHYSICS WITH NEUTRONS

Nowadays many interesting issues in particle physics and cosmology can be investigated at the lowest extremes of the energy scale, using cold neutron beams with energies from the meV down to the nano-eV range. This is due to the incredibly high sensitivity that neutron experiments can reach at these energy scales when a large number of neutrons can be stored in vessels for times approaching the lifetime of the free neutron.

Among these topics (for a full review see, e.g. [28]), it is worth mentioning

- the nature of time reversal non-invariance and the origin of the cosmological baryon

asymmetry, i.e. CP (hence T) violation: detailed investigation of neutron  $\beta$ -decay (search for T-odd correlation coefficients);

- again the possibility of a CP-violation "stronger" than the CKM matrix (and strong enough to justify baryon asymmetry) would lead to an observable Electric Dipole Moment on ultra cold neutrons of the order of  $10^{-27} e \text{ cm}$ ;
- the nature of the electroweak theory and the origin of parity violation, which is commonly called the left-handedness of nature: measurement of right-handed amplitudes in neutron decay give an upper limit on the mass of right-handed W bosons;
- again the search for exotic  $\gamma$ -less neutron decay  $n \rightarrow H \nu$ : one of the four H hyperfine states cannot be populated at all if the neutrinos are completely left-handed);
- the question of charge independence of nuclear forces implies a model-independent estimate of the neutron-neutron scattering length  $a_{NN}$ : is a direct measurement possible?

Of course, such experiments demand for a high-flux, continuous or pulsed, neutron sources such as research reactors or high power spallation facilities and cannot be performed on a electron-Linac-based source.

But there exceptions: for instance, it is worth mentioning another interesting experiment to be realized on a neutron facility, i.e. the test of additional short range forces with neutron scattering off heavy nuclei. In some theoretical schemes the presence of extradimensions may reveal as stronger space dependence of gravity at compactification distances which are of the order of a few tenth's of Fermi, so in principle distinguishable from nuclear force [29]. For this kind of activities a neutron beam with energies of  $\sim 1 \text{ keV}$  is best suited, such as the one from a moderated source.

### **3. Present and future neutron TOF facilities**

*European facilities and networks* The main facilities for differential cross-section measurements of interaction data at energies below 20 MeV are at the European Commission's Joint Research Centre laboratory, the Institute for Reference Materials and Measurements (IRMM) at Geel in Belgium. Waste handling and waste transmutation (including waste management facilities) are the major topics for the Commission's VI Framework Programme. Measurements relating to the development of new innovative reactor concepts are also being undertaken. Interest is slowly shifting to higher energies. But the energy range accessible at Geel ( $< 20 \text{ MeV}$ ) is still the most important. The refurbishment of the linear accelerator GELINA is still going on, the Van de Graaff having already been refurbished.

The n-TOF facility at CERN is partly funded by the European Commission. The measurements here complement those at Geel, and there is close collaboration between the two laboratories. Both facilities have comparable average neutron fluxes below 10 MeV, but n-TOF has a peak flux a factor of 1000 higher. The CERN facility is thus ideal for measurements on radioactive samples, but due to its high peak flux, transmission measurements cannot be made there. Measurements of capture cross-sections are made at CERN, while total cross-sections are measured at Geel. CERN's n-TOF has a lower duty cycle than GELINA, the total flux of the two machines being similar.

In addition to IRMM and n-TOF, laboratories endowed with Van de Graaff facilities are at the Instituto Tecnológico e Nuclear (ITN) in Lisbon, at the Centre d'Etudes Nucleaires (CEN) of CNRS-IN2P3 on the Bordeaux-Gradignan site, at the Stellar Nucleosynthesis Group at IK3/Forschungszentrum Karlsruhe (FZK), and at the Legnaro National Laboratories (LNL). At the Physikalisch-Technische Bundesanstalt (PTB) at Braunschweig, measurements are made of neutron activation cross-sections and of neutron scattering cross-sections (differential and double-differential) between 6 and 15 MeV using an energy-variable compact cyclotron and neutron time-of-

flight spectrometer. There is also a Van de Graaff accelerator used for producing monoenergetic neutrons and high-energy photons.

In the neutron beam facility at the proton cyclotron of the Svedberg Laboratory at the University of Uppsala, Sweden, monoenergetic neutron interaction measurements are carried out. Studies are made of neutron-proton scattering, charge exchange (n,p) reactions in nuclei, neutron elastic scattering on nuclei and fast-neutron fission dynamics.

As a new European facility for nuclear data, one has to mention the neutron sources at Forschungszentrum Rossendorf near Dresden (FZD), which exploits both the low energy, high-intensity electron beam from the ELBE SC Linac to produce an intense, white spectrum, neutron flux and a 14 MeV neutron beam from a D-T fusion generator, which cover the whole spectrum for fusion research.

The above mentioned and other minor European facilities are member of the EFNUDAT project which is an Integrated Infrastructure Initiative (I3) funded under the 6th framework programme (FP6), for nuclear data measurements and joint research activities. The main objective of EFNUDAT is to promote the coherent use and integration of infrastructure related services via networking and transnational access to the participating facilities. No Italian facility is involved. There are several other facilities, including Van de Graaff accelerators, which are being used for relevant differential cross-section measurements. A number of facilities is available for making measurements at 14 MeV. Some of these are used for studies relating to activation and heat generation in fusion materials.

There are also some facilities for studies at energies above 20 MeV. At the Université Catholique de Louvain (UCL) in Belgium, a cyclotron is used for neutron interaction measurements in the energy range 25 to 70 MeV. Measurements of double-differential cross-sections for light charged particle emission, e.g. (n,px), in neutron-induced reactions on both light materials (C, Al, Si) and heavy materials (Fe, Co, Pb, Bi, U-nat) have been completed recently.

*Non-European facilities* In Russia, at the Institute of Physics and Power Engineering in Obninsk, there are a number of facilities:

- A Van de Graaff, providing a continuous or pulsed beams of protons or deuterons, producing monoenergetic or broad spectrum neutrons.
- A cascade accelerator of protons or deuterons producing monoenergetic neutrons.
- A tandem accelerator of protons or deuterons producing monoenergetic neutrons.
- A 14 MeV neutron source, pulsed or continuous.
- A 30 MeV electron accelerator.

Recent measurements include the fission cross-sections of Cm isotopes, fission product yields in  $^{232}\text{Th}$  and  $^{237}\text{Np}$ , delayed neutron yields and relative abundances as a function of incident neutron energy, prompt fission neutron spectra, and total cross-sections and inelastic scattering.

At the Frank Laboratory of Neutron Physics in Dubna there are two pulsed reactors which provide powerful pulsed beams of neutrons, a sub-critical reactor driven by an accelerator, and a pulsed prompt critical reactor. Recent measurements include delayed neutron yields. It is planned to build a new high-flux facility, INES.

In Asia, facilities operated by JAERI include the 14 MeV Fusion Neutronic Source (FNS) and a 20 MV tandem accelerator providing monoenergetic neutrons in the ranges 9-13 and 17-30 MeV. Recent measurements include activation cross-sections around 14 MeV and secondary neutron and gamma spectra for integral benchmark experiments. In collaboration with the High Energy Accelerator Organisation (KEK) in Tsukuba, a multipurpose intense proton accelerator complex (J-PARC) is being built which will include an intense spallation neutron source for neutron scattering. Proposals are being made to the project to install beam lines and/or targets suitable for nuclear data

measurements from thermal to the GeV region. If equipped in this way the accelerator and neutron source will be very useful for nuclear data measurements.

Several other facilities are located in Japan (Tohoku University, Tokyo Institute of Technology, Department of Nuclear Engineering and Nuclear Science of Osaka University, Research Reactor Institute of Kyoto University) which cover a vast field of applications in neutron research.

At the China Institute of Atomic Energy there is a tandem Van de Graaff accelerator producing pulsed beams of deuterons and protons from which neutrons are produced using deuterium or tritium gas targets. There are also facilities at Peking University Institute of Heavy Ion Physics (Van de Graaff), at Sichuan University and at Lanzhou University (14.7 MeV). Measurements have been made of double-differential (n,n) and (n, $\alpha$ ) cross-sections, activation cross-sections, gamma spectra and fission product yields.

Last but not least, we must cite the recent neutron facility at the POHANG Laboratory in South Korea [30], based on an expressly built electron Linac and developed in collaboration with Japan, which has already provided very valuable measurements for nuclear industry.

In USA, at Los Alamos National Laboratory (LANL) the Neutron Science Center (LANSCE) has two spallation sources. At the WNR facility the neutrons are un-moderated and range from about 100 keV to 800 MeV. At the Lujan Center the neutrons are moderated and range from sub-thermal to about 100 keV. There are a number of flight paths for the time-of-flight measurements at each source. Including all of the capabilities, nuclear data measurements can be made over 16 orders of magnitude in neutron energy.

A number of enhancements have been made in recent years. The emphasis of the measurements recently made has been on total cross-sections for a range of materials in the energy range 5 to 560 MeV to an accuracy of 1% or better, and on (n,x $\gamma$ ), (n,xp) and (n,x $\alpha$ ) cross-sections to several hundred MeV. Comprehensive fission measurements have also been made in recent years, together with a new capability to measure fission prompt neutron spectra. Measurements of neutron-capture cross-sections of radioisotopes have begun. There is funding for work relating to the transmutation of waste, including requirements for advanced applications for accelerator transmutation studies.

Another major spallation source is the Intense Pulsed Neutron Source (IPNS) at the Argonne National Laboratory, which provides a much lower intensity than LANSCE, but with better time resolution.

At Oak Ridge National Laboratory (ORNL) there is the pulsed- white spectrum- TOF facility of ORELA electron linear accelerator with energies ranging from sub-thermal to 80 MeV. Improvements have recently been made to the neutron capture measurement facility. Recent measurements

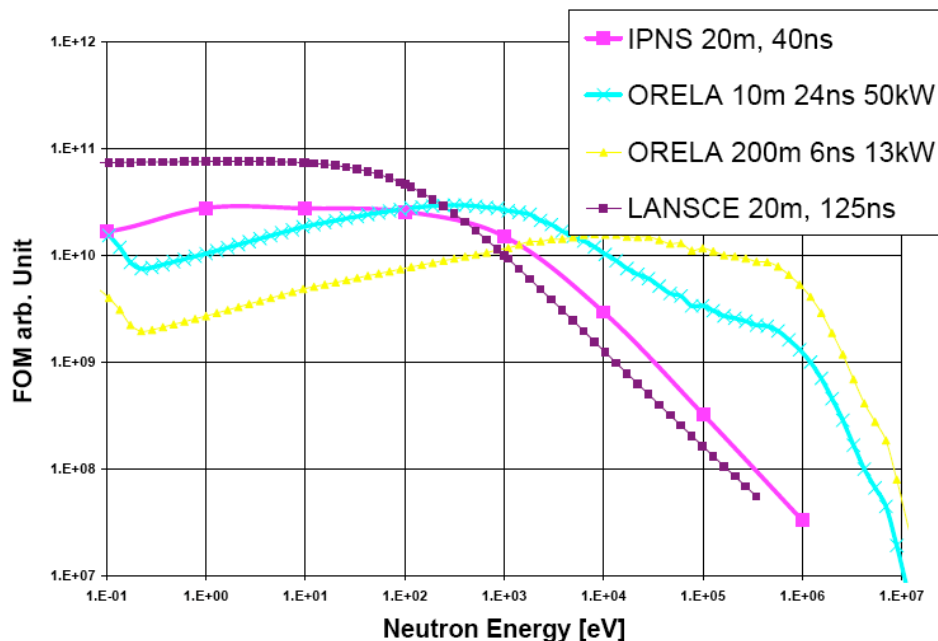


**Figure 10 Comparison of figures of merit (neutron flux divided by the square of the resolution vs. neutron energy) for the different neutron sources in the USA[31]**

include  $^{233}\text{U}$  transmission and fission, Al transmission and capture, and capture in Si, Cl and K.

The new big facility, the Spallation Neutron Source (SNS) came into operation in 2006, with a total cost US\$1.4 billion. This is using a mercury target and a beam of 1 GeV protons, providing the most intense neutron beam in the world. Although this facility will concentrate on neutron scattering for condensed matter research, one beam line is being proposed for nuclear data measurements and another for fundamental physics measurements.

At the Rensselaer Polytechnic Institute the Gaertner Laboratory linear accelerator facility has recently been refurbished. Neutron transmission and capture measurements have been made for Cs, Sm,  $^{155}\text{Gd}$  and  $^{157}\text{Gd}$ , and transmission for  $^{236}\text{U}$ . At the University of Massachusetts Lowell there is a pulsed Van de Graaff accelerator which produces monoenergetic neutrons. Neutron elastic and inelastic scattering and total cross-sections are being measured. Recent work is  $^{159}\text{Tb}(n,n'\gamma)$  below 1 MeV and total cross-section measurements for  $^{235}\text{U}$ ,  $^{159}\text{Tb}$  and  $^{169}\text{Tm}$  from 200 to 400 keV. At the Colorado School of Mines there is a small Cockroft-Walton accelerator used to generate nuclear data for astrophysics, mainly regarding low-energy proton and deuteron reactions on very light nuclei.

There is close co-operation both nationally and internationally between scientists working in the different laboratories, with the facilities being used by international teams.

*Capability of satisfying current data needs* Despite the large number of experimental facilities, especially in Europe, the world's capability of satisfying current data needs is quite limited. Indeed, most of them are not much used for measurements of nuclear data for nuclear energy-related issues. Operation of these facilities is expensive and expertise is limited. So the use of synergies with International Initiatives, like I3 and Transnational Access programmes in Europe is welcome. At NEA there's a Research and Test Facilities Database (RTFDB), similar to the NDS at IAEA. This database, set up by the NEA Expert Group on Needs of R&D Facilities in Nuclear Science, was established as

part of the expert group's worldwide review of the status of research and test facilities in the field of nuclear science and technology.

*Ensuring the continuity of facilities and expertise* The High Priority Nuclear Data Request List shows that there is a continuing and important need for high-accuracy nuclear data measurements. However, the number of scientists working in this field has declined over the past 20 years, and many differential and integral measurement facilities have been shut down. In Western Europe, there is a new facility at CERN. However, the measurements being made at CERN relating to nuclear technology applications, and those at IRMM in Geel, are funded by the European Commission, and there is no guarantee that the funding for these will continue long into the future. University nuclear physics departments have made a major contribution in the past, and their input remains significant. However, nuclear data is no longer regarded by some younger researchers as at the frontiers of nuclear physics research. It can be anticipated that the contribution from universities will decline, making it necessary to consider how it can be replaced in the future. This trend is also a problem for recruiting well-trained researchers to replace those who retire.

In the USA, an important contribution is made by retired scientists who continue to make measurements and carry out research on a part-time basis. In France, retired scientists are also encouraged to play a part in guiding junior scientists and to participate in research. It is less common for retired scientists to be provided with the necessary facilities in other countries, except in universities. In some countries (an example being France) an effort has been made to train young scientists to ensure that the necessary expertise is maintained. Other countries might consider similar schemes. There are several programmes which are monitoring the situation. Examples include the initiative being undertaken by the NSC and the FRAMATOME project on "Nuclear Expertise and Research Facilities in Europe".

*Importance of having a national neutron TOF source* In Italy, the neutron sources are quite old and scarcely used for research purposes. There are presently only 4 low power reactors, the 2 TRIGA Mark II reactors, one (RC-1) at ENEA-Casaccia and the other (LENA) at the Univ. of Pavia, the homogeneous reactor AGN (Aerojet Gen, Nucleonics) at the Univ. of Palermo, the TAPIRO fast source at ENEA-Casaccia, plus a few D-D and D-T fusion sources. None has capability for nuclear TOF data production.

After the 20-years-long 'antinuclear winter', which followed the results of the post-Chernobyl referendum in 1987, the need for re-starting the research also in this field has been stressed several times, in the scientific and political meetings. Quite limited efforts were put in until now, which pointed mainly at strengthening the Italian collaboration with the CERN n-TOF facility, but didn't produce any significant result as far as the development of national facility is concerned. Investments have been poor, amounting to a few M€ for the whole fission programme from ENEA and ~ 7 M€ for the ADS research (TRASCO programme) from MIUR-INFN-ENEA, for the construction of the RFQ injector prototype at LNL, in Padua. There the big project SPES (Selective Production of Exotic Species) includes also a neutron powerful source, which couldn't be used anyway for TOF measurements, once built.

The Italian participation in the international programmes is certainly valid at the individual level, but very scarcely supported by the national institutions: besides some participations in international committees and working groups, without any direct involvement in real activities, except for the EUROTRANS (Waste Transmutation) and ELSY (European Lead-cooled System) programmes in the fission sector, but not at all in the EFNUDAT network, nor in the CANDIDE (Coordination Action on Nuclear Data for Industry Development in Europe) initiative.

The Italian participation in foreign-based experimental activities (practically only the CERN n-TOF) cannot be sufficient to recover the necessary level of expertise and knowledge which the country was endowed before, nor the presence of Italian scientists and engineers in some high-level international committees and foreign research institutes (such as the CEA in France and ANL in U.S.)

can be deemed sufficient to that purpose.

## **4. The neutron source**

### **4.1 OVERVIEW OF THE FACILITY**

As already suggested by some authors [32, 33] the realization of an  $e^-$  Linac – based neutron facility still appears a viable option for high resolution measurements of energy dependent cross-sections with the time-of-flight (TOF) technique. This is because the real figure of merit for many experiments is not just the maximum attainable flux, but the flux at a given energy resolution, which is basically dependent on the arrival time spread of the primary beam and on the artificial pathlengthening of neutron within the radiating target.

Hereafter the advantages of using an electron beam appear quite evident, as compared with a primary hadron (proton, deuteron) beam: much shorter bunchlength, much smaller source size, hence possibility of reduced pathlength for TOF measurement, what allows to keep the flux at an acceptable level with good energy resolution. Last but not least, the possibility of running the neutron source as a post-product of electron acceleration seems very appealing, if the Linac is devoted to some beam-non-destroying application such as the Free Electron Laser (FEL). The efficient use of a non-dedicated facility for secondary beam production is again an advantage over hadrons, not to mention the reduced cost of an electron machine.

Another non-negligible advantage of this source is the high energy primary beam: the neutron production strength depends only on the beam power, at least above a certain threshold and for heavy metal targets. But at a given beam power, it is better to have higher energy and lower current than the opposite, because the density of thermal power deposition in the target is more dilute along the target's length, so less critical for the target's thermal stability, as we shall see in a next paragraph.

Therefore the neutron source is conceived as an end product of an electron beam, whose main purpose is the realization of a X-ray FEL Facility in the Rome Research Area, but in such a way that it might be tested and implemented also on the injector Linac of the double annular 500 MeV electron-positron Storage Ring DAΦNE at Frascati Natl. Labs (LNF) of INFN.

The X-FEL initiative (named SPARX) is a joint project carried on by scientists and engineers of the major Italian research institutes and strongly supported by the Italy national and Latium regional governments. Its various articulations are described in the literature extensively [34, 35].

For our purpose here we just remark that the superconducting option for the final Linac (energy = 2.5 GeV), by allowing a much higher average power [36], would clearly open more possibilities of experimental research, not strictly confined to the SPARX programme.

While the path to the final goal of the SPARX project is still very long, a ‘day one’ option might also be the installation of the neutron source on the LNF Linac. The Linac is presently devoted to the injection of DAΦNE, what is the main part of the accelerator complex at Frascati, and is also feeding a Test Beam Facility (BTF), where first tests can be performed. However, this one cannot be a definitive location for the neutron source, owing to the tight limits imposed on the electron beam intensity by safety regulations, which are presently set at only  $10^{10}$  electrons/sec.

A more interesting possibility is the installation of the neutron radiator directly in the tunnel of the DAΦNE linac, whose maximum average power is  $\sim 1$  kW, while its typical value for the injection mode is  $\sim 60$  W. Incidentally, we may note that the Linac, when running in the positron operation mode with converting target extracted where the gun current can be pushed up to 7 A, is able to

deliver more than 2 A per pulse at the energy of 510 MeV on its final end, even with some energy spread induced by the increased beam loading. Owing to these power limits from the accelerator, the neutron flightpath anyhow should be as short as just 1 m, in order to get a total flux of the order of  $10^5$  n/s/cm<sup>2</sup>. On such a short base the separation of fast neutrons from the prompt  $\gamma$ -ray flash as generated by bremsstrahlung puts a constraint on the maximum measurable energy. We shall address this problem later on, in a further study.

A comparison of the various options for this neutron source with other linac-based facilities, both long-standing, like GELINA and ORELA, and recently started, like ELBE and POHANG, is reported in Table III.

INSTITUTE Facility	IRMM Gelina	ORNL Orela	FZD Elbe	POHANG Linac	INFN-ENEA Sparx NC	INFN-ENEA Sparx SC	LNFI Linac
energy(MeV)	100	180	30÷40	100	2500	2500	510
beam power (kW)	7	8	5	~ 0.2	8	144	0.5
pulse charge(nC)			1.8		1	1.6	20
rep. rate (Hz)	800	1000	$5 \cdot 10^5$	12	100	5	50
pulse length (ns)	1÷10	2÷24	0.002÷0.01	1800	0.01	0.01	10
flightpath (m)	10	9	4	12	1	1	1
Source strength (n/s)	$3.4 \cdot 10^{13}$	$10^{14}$	$2.7 \cdot 10^{13}$	$4 \cdot 10^{11}$	$1.7 \cdot 10^{13}$	$3 \cdot 10^{14}$	$1.0 \cdot 10^{12}$
Flux/lethargy (#/s/cm <sup>2</sup> ) at 1 eV	$4 \cdot 10^4$	$10^4$	$4 \cdot 10^5$	$0.5 \cdot 10^3$	$\sim 10^6$	$>10^7$	$10^5$

**Table III Old and new facilities vs. various options for a neutron source at INFN [37]**

## 4.2 THE NEUTRON RADIATOR

Unlike most accelerator neutron sources, where the neutron radiator is very well separated from bunker wall and other materials, in order to minimize background, here the design was adopted of integrating the neutron radiator inside the beam dump, quite similar to the ELBE [38] radiator. This choice was due to the requirement of having maximum intensity from the target, hence to the need of putting the experimental measuring station as closer as possible to the target. So a reference minimum distance of 1 m was chosen, in order to get an acceptable flux of  $10^5$  n/s/cm<sup>2</sup> at the lowest available source strength. This means that an efficient screening system has to be implemented, to reduce significantly the huge background field that would make the use of any detector almost impossible, besides producing undesired activation of equipment and materials that are located in experimental hall.

Certainly, it is a common and safe practice to avoid the presence of much heavy material around the target, because of the additional background, mainly due to scattered low energy neutrons from the beam dump and collimator walls.

In this case, owing to the low power (< 1 kW) of the primary beam, a special design has to be adopted, aiming at minimizing all background sources (fig. 11). The main problem here is the huge  $\gamma$ -flash coming from bremsstrahlung on the target, what makes the use of heavy metal shielding almost

mandatory. Then an adequate thickness of light hydrogenated material is necessary to moderate the big number of neutrons.

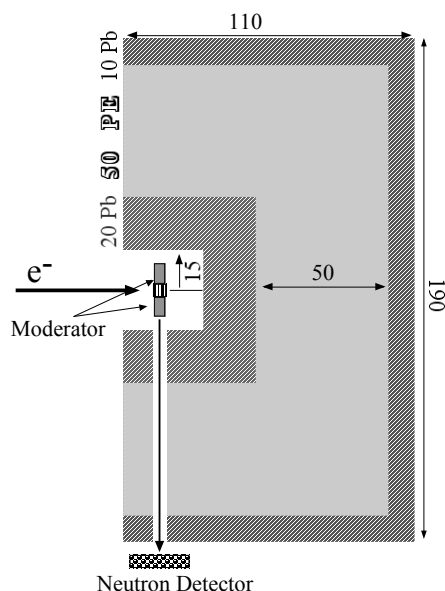


**Figure 11 The basic structure of the radiator shielding system and beam dump**

The main items of the optimization work are the target geometry and thermal behaviour, the moderator materials and the general design of target shielding and beam dump.

### 4.3 TARGET DESIGN

The high level of power deposition does not allow, in most of high power accelerators, a simple mechanical design or the use of solid metal for the neutron producing target. This is particularly true when the neutron yield, which is basically a function of the beam power only, is produced mainly by acting on the beam current rather than on the beam energy. So in case of high energy electron beams, the requirements on the power dissipation are less stringent, since the energy loss in thick targets is more gradual and is distributed longitudinally on a larger volume. The target radius instead, which has little influence on the neutron intensity, has to be kept small, since it is rather influent on neutron path from generation to detection, i.e. on the energy resolution. For low energy electrons, instead, the energy loss in thick targets concentrates in the very first path, thereby favoring high energy vs. low energy beam [39].

It is worth noting that the in case of spallation sources the target size has to be much larger, owing to the bigger size of the hadronic cascades compared with the electromagnetic ones. As an example, according to the well know parametrization of e.m. and hadronic showers [40], the radius and length of cylinder target have to be  $R=2.5$  cm,  $L=6.15$  cm and  $R=11$  cm,  $L=35$  cm, for the 1 GeV  $e^-$  and 1 GeV proton beams, respectively, to ensure a full containment of cascade energy. So, since the

energy resolution is strongly affected by target radius, this fact suggests that the electron-driven sources are certainly not inferior to spallation sources, at least for time-of-flight measurements.

A theoretical description of the resolution function for neutron TOF sources will be given in §4.9. To the actual purpose, it is important to stress that the optimization of the target was performed by keeping the resolution in the intermediate energy region as the leading criterion. As already said, a radius of  $R = 2.5$  cm will ensure the full containment of beam energy, but a smaller radius is still acceptable, provided the neutron source strength is not reduced by more than 5-10% and the energy resolution is correspondingly increased. A full simulation campaign with MCNP5 [41] was done, assuming a cylindrical compact Ta target, 6.15 cm long (equivalent to 15 radiation lengths) and variable radius from 0.75 up to 2.5 cm

For sake of completeness, the resolution function was studied for two cases: point-like beam (no space-time structure), what is useful for the assessment of the source features, and gaussian-shaped beam with  $\sigma_{x,y} \approx 2$  mm and  $\sigma_t \approx 1$  ns, useful for comparison with other TOF facilities. For this preliminary study neither moderator nor shielding were included.

In table IV the neutron strengths, i.e. the number of neutrons per primary electron are reported for 4 different target radii.

	0.75	1.0	1.5	2.5	Conical 0.75-2.5	Swanson formula
pencil beam	0.274	0.295	0.312	0.321	-	0.328
gaussian beam	0.264	0.289	0.309	0.321	0.307	0.328

**Table IV Source strength (n/e<sup>-</sup>) for various target radii (cm)**

The case of  $R=0.75$  is discarded, since the dropping in neutron strength is clearly too large, and it is not compensated by a significant improvement in resolution, while the other 3 cases are kept since their strengths are within 10% of the maximum theoretical value as computed with Swanson's formula for semi-infinite target [42].

The resolution for the 4 target radii is compared in the Fig. 12 for the pointlike beam in the 4 most significant energy regions, between 1 keV and 10 MeV. The resolution is expressed as function of the 'delay distance', i.e. the neutron pathlengthening with respect to its nominal value  $L$ , as originated by scattering and interaction in the various traversed materials.

A general feature of these distributions is the peak shifting towards increasingly positive values of delay distance with increasing energy, what is due to scattering process inside the target itself. The lower energy regions are indeed populated by neutrons which either are unscattered, off-axis generated neutrons or have scattered once in the target and lost most of their initial energy before detection. Under these conditions the delay distance may be negative, as in the more obvious case of off-axis unscattered neutron generation, while at higher final energy the percentage of energy lost during scattering process decreases and only the pathlength increases, as it happens for most high-Z materials. As a further consequence, a remarkable broadening of the peak curves is also observed with increasing energy, while the positive tail becomes steeper for smaller target radius, as expected.

The difference between the  $R=1$  cm and the  $R=2.5$  cm targets is impressive, particularly at energies below 100 keV, where the presence of multiscattering particles in the larger target increases the asymmetry considerably. At higher energies instead, the probability of scattering becomes lower ( $\sigma \sim 1/v_n$ ), so the difference in the target size has less influence.

For the gaussian beam the resolution in all significant energy regions are displayed in Fig. 13, which confirm a clear preference for the  $R=1$  cm case and exhibit an enhancement of the peak broadening vs. neutron energy.

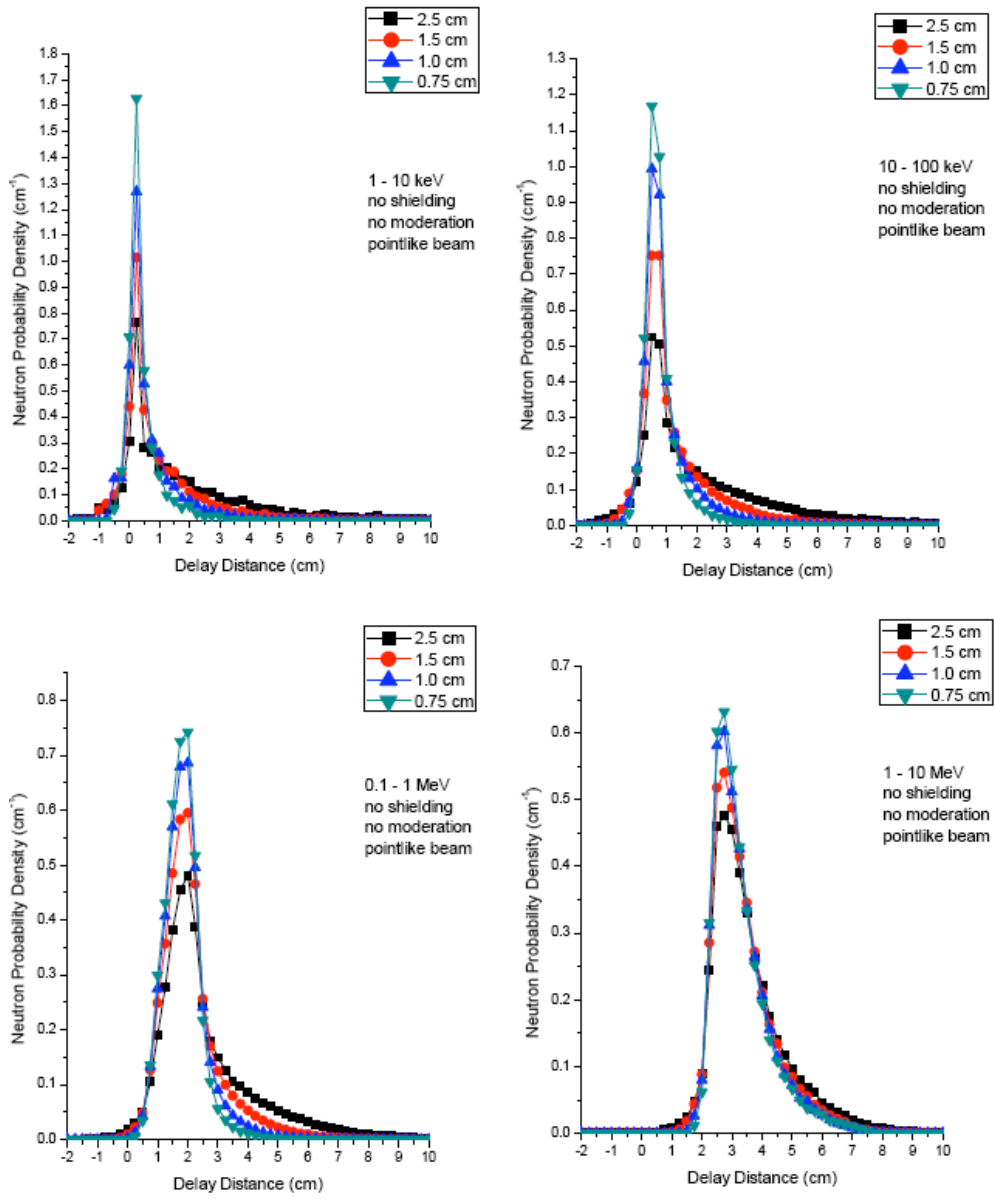
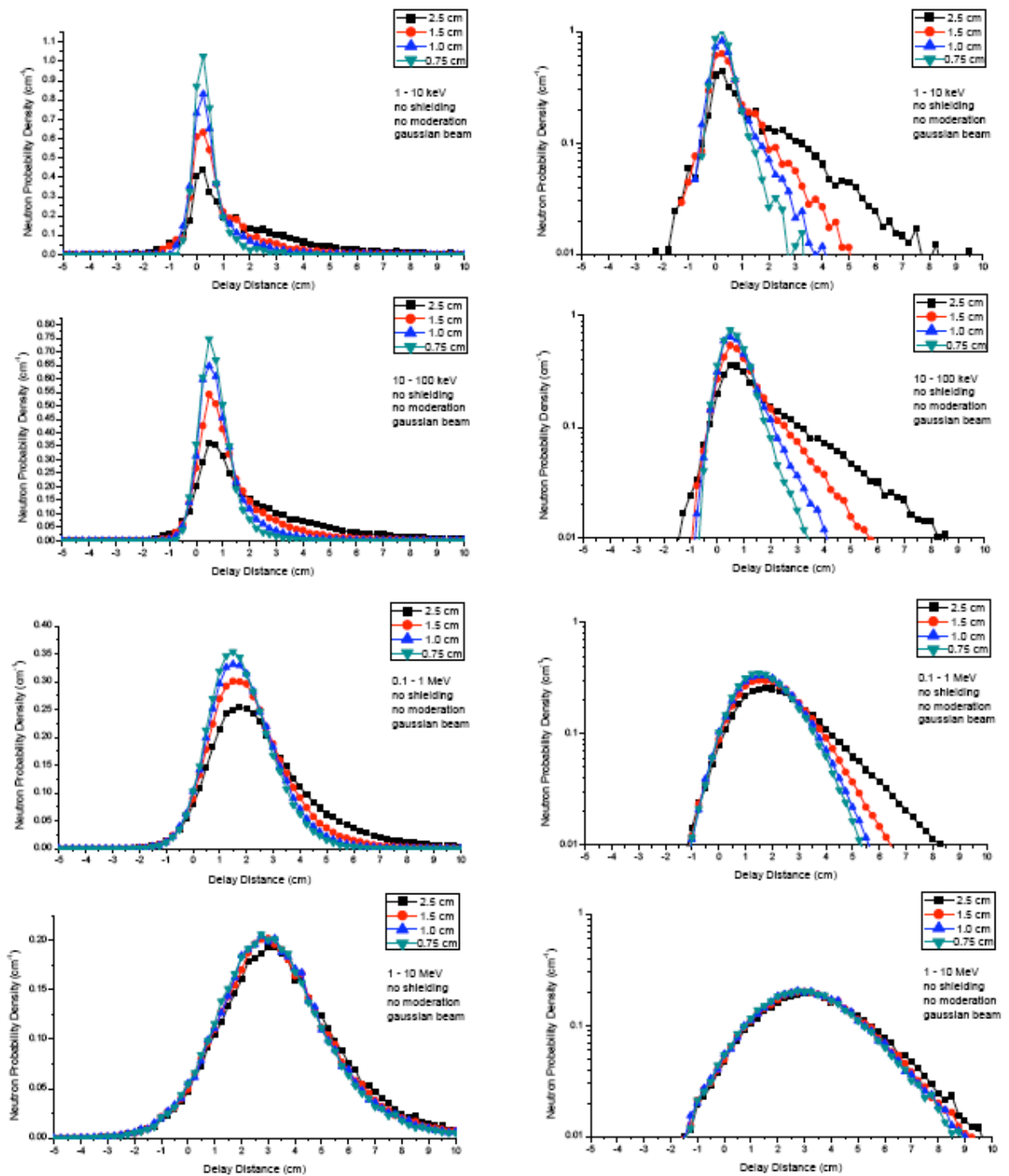
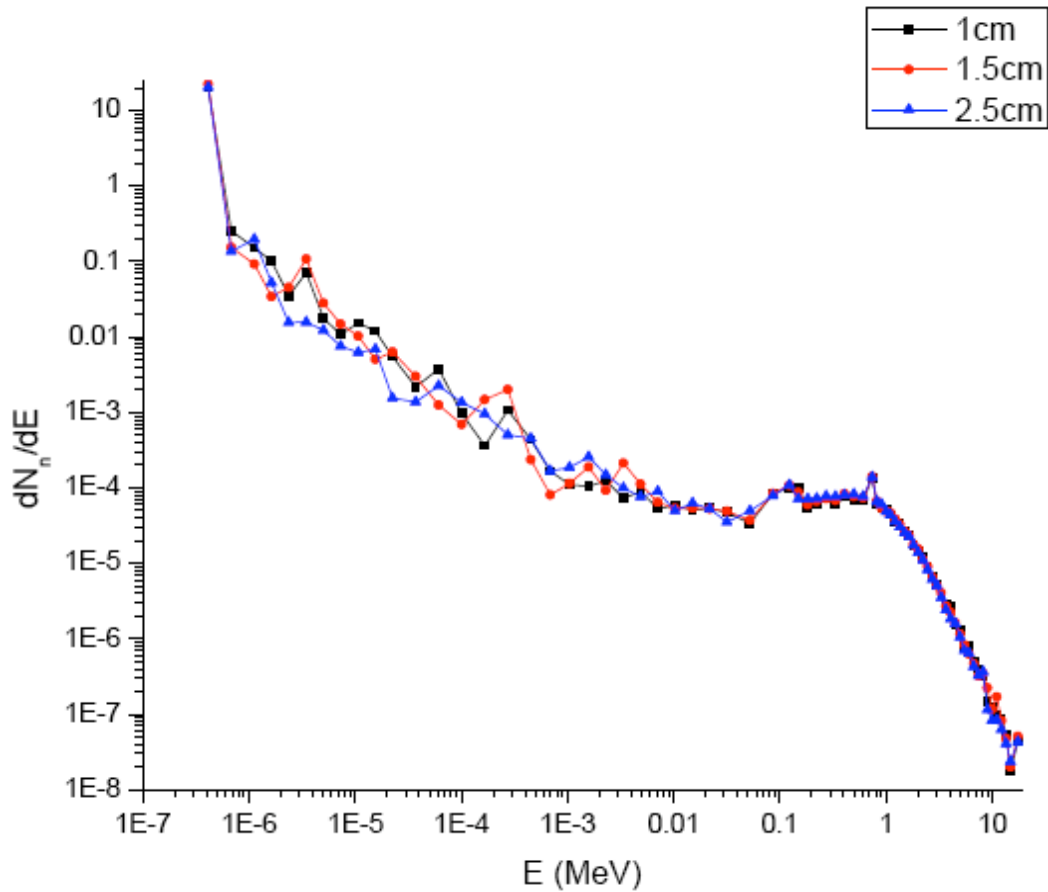


Figure 12 The delay-distance distribution for various Tantalum targets



**Figure 13** The delay-distance distributions for a gaussian beam and various Ta targets (left linear, right logarithmic plot)



**Figure 14** The direct neutron spectrum for three target radii.

The neutron spectrum for all the considered targets is shown in fig. 14.

As a further optimization check we have also considered the possibility of using a target of different shape, like a truncated cone, which takes into account the progressive spread of the e.m. shower. (Moliere radius). The resulting neutron strength for the gaussian beam is not significantly lower than the one from a cylindrical target (see Table IV), as it is dependent mainly on the target length. A sketch of this target and the resulting RF are shown in figs. 15 and 16, respectively.

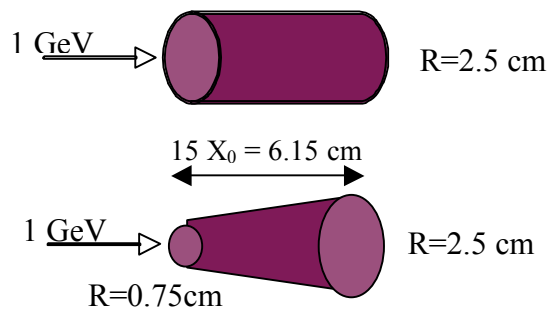


**Figure 15** The truncated cone vs. the cylindrical target

A remarkable improvement is observed everywhere, except on the higher part of the spectrum, where scattering effects become less significant ( $\sigma \sim 1/v_n$ , again).

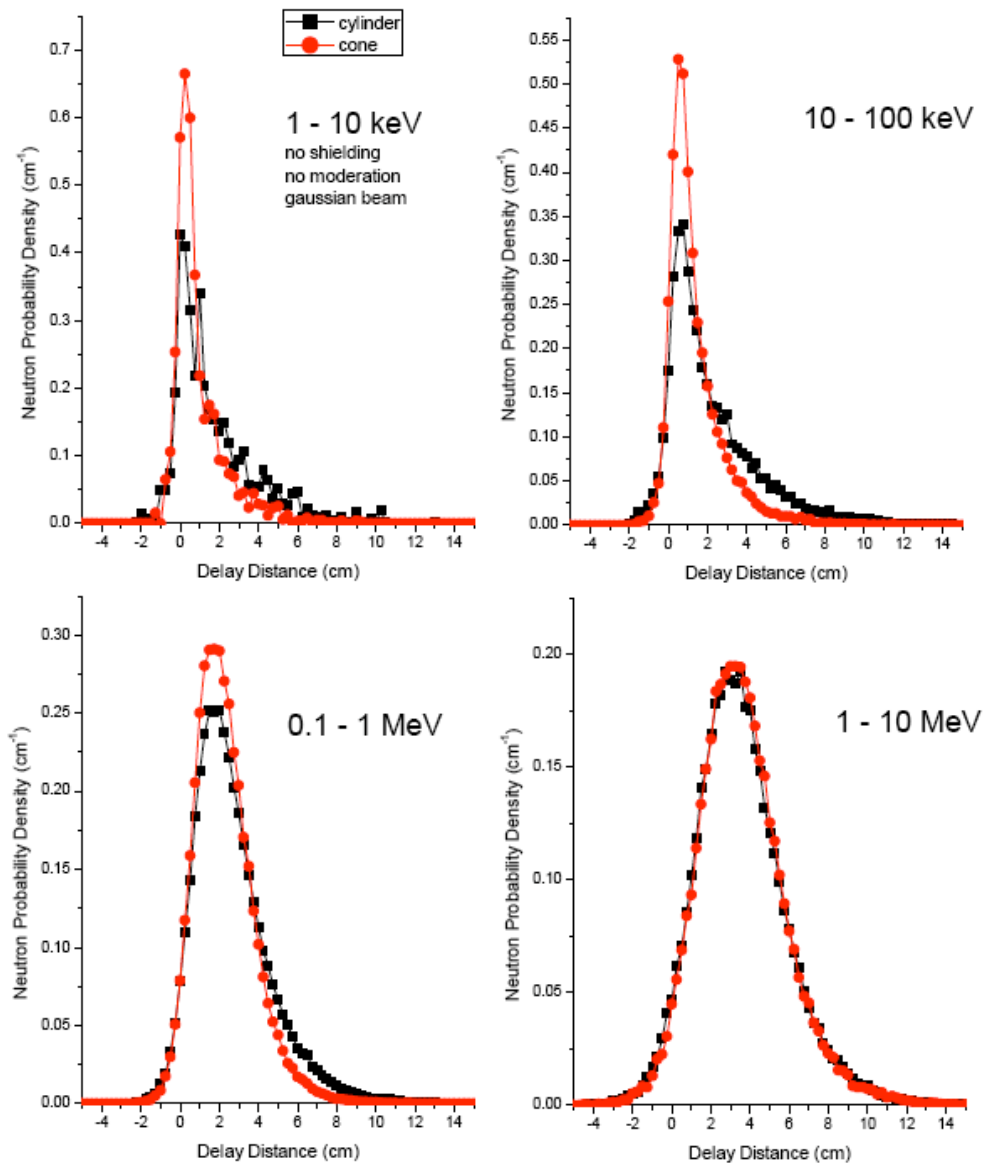
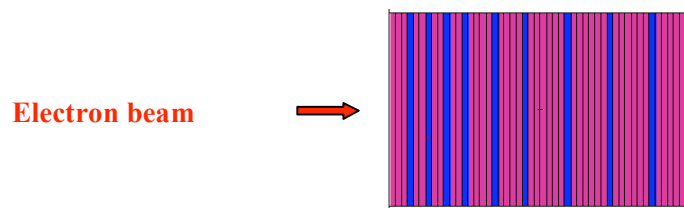


Figure 16 Delay distance distribution: comparison between a cylindrical and a conical-shaped target for a gaussian beam

#### 4.4 THERMAL BEHAVIOUR

Unlike most high-power facilities, the problem of target heating and stability against thermal stresses is not critical, since the maximum beam power won't overcome 1 kW. Nevertheless, the final target design will include a cooling system, which can be made of simple pure water when the target is operated with moderator, or some high-A material, like Mercury or molten Lead, when the direct spectrum is used, to avoid any undesired perturbation. As for the previous simulations, a cylindrical Tantalum target was adopted, made of plates of various thicknesses, each 1.5 mm apart to allow for cooling and arranged in a cylinder of 2.5 cm radius and  $15 X_0$  length (6.15 cm). The MCNP simulations were done for a target model made of 10 Ta plates, 4.5, 3, 3, 3, 4.5, 6, 9, 9, 9, 10.5 mm thick with 1.5 mm of void between them,  $R=2.5$  cm. This target model is sketched in fig. 17.



**Figure 17 The target model for thermal calculations**

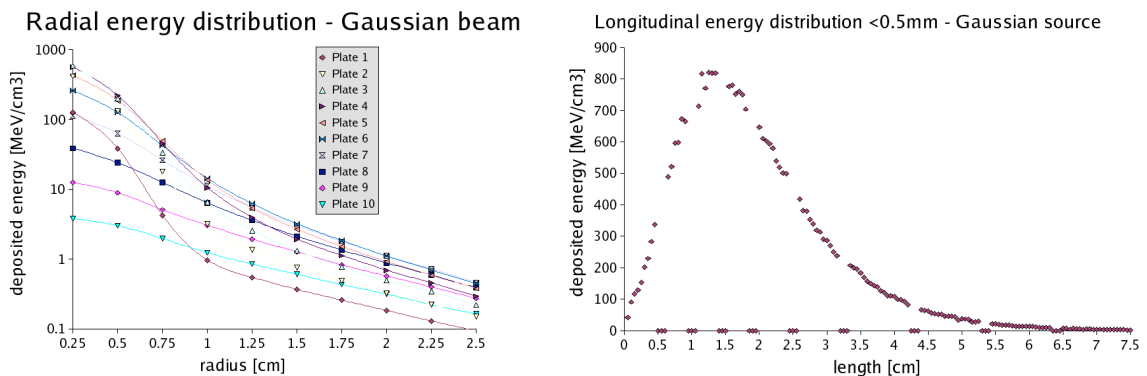


**Figure 18 Radial and longitudinal (on-axis) density of deposited energy in the target at 1 GeV (stepsize 0.5 mm)**

The radial and longitudinal energy deposition in this target are displayed (Fig. 18) for a gaussian source with  $\sigma_{x,y} \approx 2$  mm. We used the actual beam spot size of BTF at maximum energy as the reference values for beam parameters and we keep  $E = 1$  GeV as our reference energy.

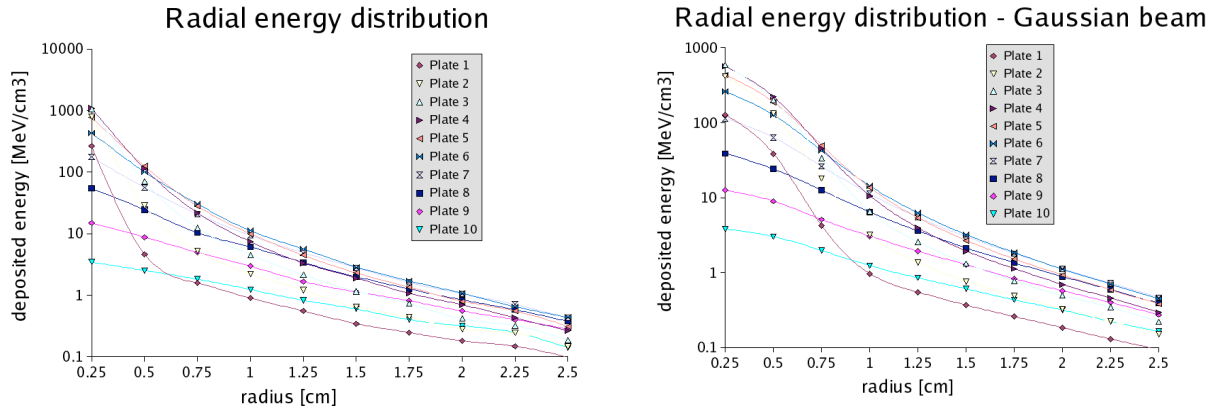


**Figure 19 Radial distribution of the deposited energy per unit volume, pencil beam (left) and gaussian beam (right) for every plate**

In fig. 19 the radial distribution of the deposited energy per unit volume is compared for the two cases, pencil beam (left) and gaussian beam (right) for every plate. The point at  $R=0.25$  cm corresponds to the average energy per particle deposited within the volume limited by that radius and the plate length. Even in case of pencil beam the power density is not bigger than  $1 \text{ kW/cm}^3$  ( $1 \text{ MeV} = 1\text{W}/1\text{mA}$ ) for a  $1 \text{ kW}$ ,  $1 \text{ GeV}$  beam. The possibility of a local 'thermal bump' was also considered, by running with a finer step ( $0.5 \text{ mm}$  instead of  $1.5 \text{ mm}$ ), but the situation doesn't change significantly for the gaussian beam, as depicted in fig. 18.

The maximum density stays well below  $1 \text{ kW/cm}^3$  at  $1 \text{ kW}$  power in the beam, what can be considered a safe value, according to a common experience for solid metal targets [43].

A rough estimate of the temperature rise in the target can be made by assuming a cylindrical geometry for the target and looking at the conduction through a cylindrical wall in steady condition. By definition of  $k$  (thermal conductivity of Ta  $k=57.5 \text{ W/m/}^\circ\text{K}$ ), the heat flow per unit area  $H$  is

$H = -k \frac{dT}{dx}$  where  $x$  is the displacement orthogonal to the surface and the minus sign means that the heat goes from higher to lower temperature zones. If a heat source is located on axis, assuming target length is much bigger than radius (almost our case) a heat flow can be defined per unit cylinder length  $H_l$  and obviously  $H_l = -k2\pi r \frac{dT}{dr}$  for the heat flow thru the surface between radii  $r$  and  $r + dr$ . Since

$H_l$  doesn't depend on the radius, by integrating this equation and we get  $H_l \int_{r_1}^{r_2} \frac{dr}{r} = -2\pi k \int_{T_1}^{T_2} dT$  for the

heat flow between  $r_1$  and  $r_2$ , and finally, for any radius  $r_1 < r < r_2$  we get:  $H = \frac{H_l}{2\pi r} = \frac{k(T_1 - T_2)}{r \ln(r_2/r_1)}$  for

the heat flow per unit area.

In practical cases we have from calculation only a power (or energy per particle)  $W$  deposited per unit target volume [ $W/\text{cm}^3$ ], and assuming it is independent of radius (quite conservatively) and uniform within a radius  $R$ , we have  $H_i = W\pi r^2$  and, substituting and integrating from a generic  $r$  to target radius  $R$ , we finally get for the temperature  $T$  at radius  $r < R$

$$T - T_R = \frac{WR^2}{4k} \left( 1 - \left( \frac{r}{R} \right)^2 \right)$$

As an example, if we know from simulation that the maximum power is deposited within 0.25 cm from axis, we can overestimate the temperature rise for  $r=0$  assuming the total power (1 kW) is deposited there and dividing by the volume ( $\pi \cdot 0.25 \cdot 0.25 \cdot 5 = 0.98 \text{ cm}^3$ ) we get  $W=1 \text{ kW}/\text{cm}^3$ , so finally  $T(r=0) = T_R + 27 \text{ }^\circ\text{K}$ , absolutely negligible. The temperature  $T_r$  can be assumed fixed as the 'external' temperature ( $= 300 \text{ }^\circ\text{K}$ ).

This is certainly a more extreme hypothesis than assuming that the whole power is dissipated uniformly in the target, but still would require a closed look if the beam size is really pencil-like at the target front.

As a comparison with the GELINA new U-target ( $k= 25 \text{ W}/\text{m}/^\circ\text{K}$ ,  $P=10 \text{ kW}$ ,  $V= 35.3 \text{ cm}^3$ ,  $R=1.5 \text{ cm}$ ) one has the average power loss  $W=0.283 \text{ kW}/\text{cm}^3$  and  $T(r = 0) = T_R + 636 \text{ }^\circ\text{K}$ , quite intolerable for Uranium even in this underestimating hypothesis [43].

So, though the power density is lower for GELINA, the higher total power and lower material conductivity make the difference.

Target cooling by water should be avoided, because the neutron spectrum is strongly affected. At this power level radiation cooling seems sufficient indeed, since a conservative estimate of heat loss through the target surface (assumed as a single Ta cylinder), at the maximum allowed  $T = 2500 \text{ }^\circ\text{K}$  and emissivity  $\epsilon = 0.1$  gives an irradiated power of  $\sim 3 \text{ kW}$ . In case of much higher beam power an appropriate cooling system must be provided, what doesn't moderate the neutron spectrum significantly

## 4.5 MODERATOR

Since a neutron beamline only is foreseen at start, the moderator is represented by an annular layer of liquid material, concentric with the target, as in fig. 4 in order to get the maximum slow neutron intensity. The neutron current per electron at 1 m distance from target centre was computed with MCNP5 for thermal neutrons ( $E < 0.4 \text{ eV}$ ), showing a maximum at a thickness of 7 cm for light water (Table V), while the maximum current obtained with heavy water is  $2.7 \cdot 10^{-9} \text{ n}/\text{cm}^2/\text{e}^-$ .

The resulting neutron spectrum is also shown in fig. 3 for 1  $\mu\text{A}$  beam current. The presence of fast neutrons is unavoidable since the beam port views the target directly through the moderator, but it can be reduced by means of time-of-flight.

The resolution function is strongly altered by the moderator, as it is clearly visible in figs. 21-a,b but even for high thickness values a FWHM resolution less than 5% seems attainable in the region below 10 keV. The shape of the RF is clearly dictated by the moderator, the target size plays almost no role, except at high energy and high delay distance, as it is confirmed by the radially observed neutron currents at 1 m distance.

**Table V The transmitted neutron current for various moderator thickness and two target radii**

Moderator thickness	Total current R=1.0 cm	Total current R=2.5 cm	E < 0.4 eV current R= 1.0 cm	E<0.4 eV current R=2.5 cm
1	9.35E-5	9.35E-5	4.71E-6	4.69E-6
3	6.75E-5	6.76E-5	8.67E-6	8.74E-6
5	4.47E-5	4.47E-5	8.88E-6	8.86E-6
7	2.83E-5	2.83E-5	6.97E-6	6.98E-6

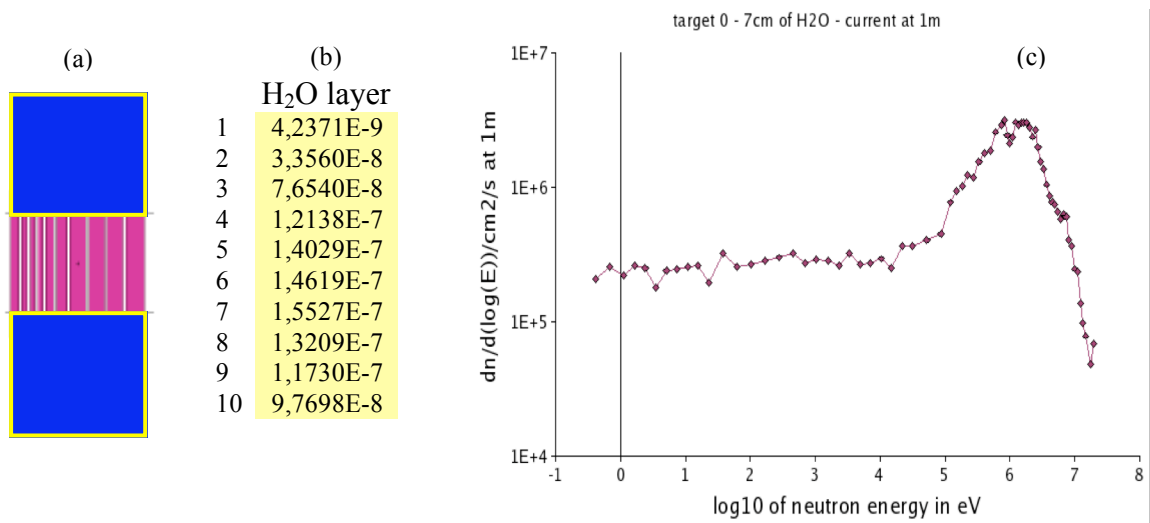


**Figure 20 The moderator optimization: (a) the target + moderator sketch, (b) the neutron current vs. moderator thickness (cm) and (c) the spectrum at the optimum thickness**

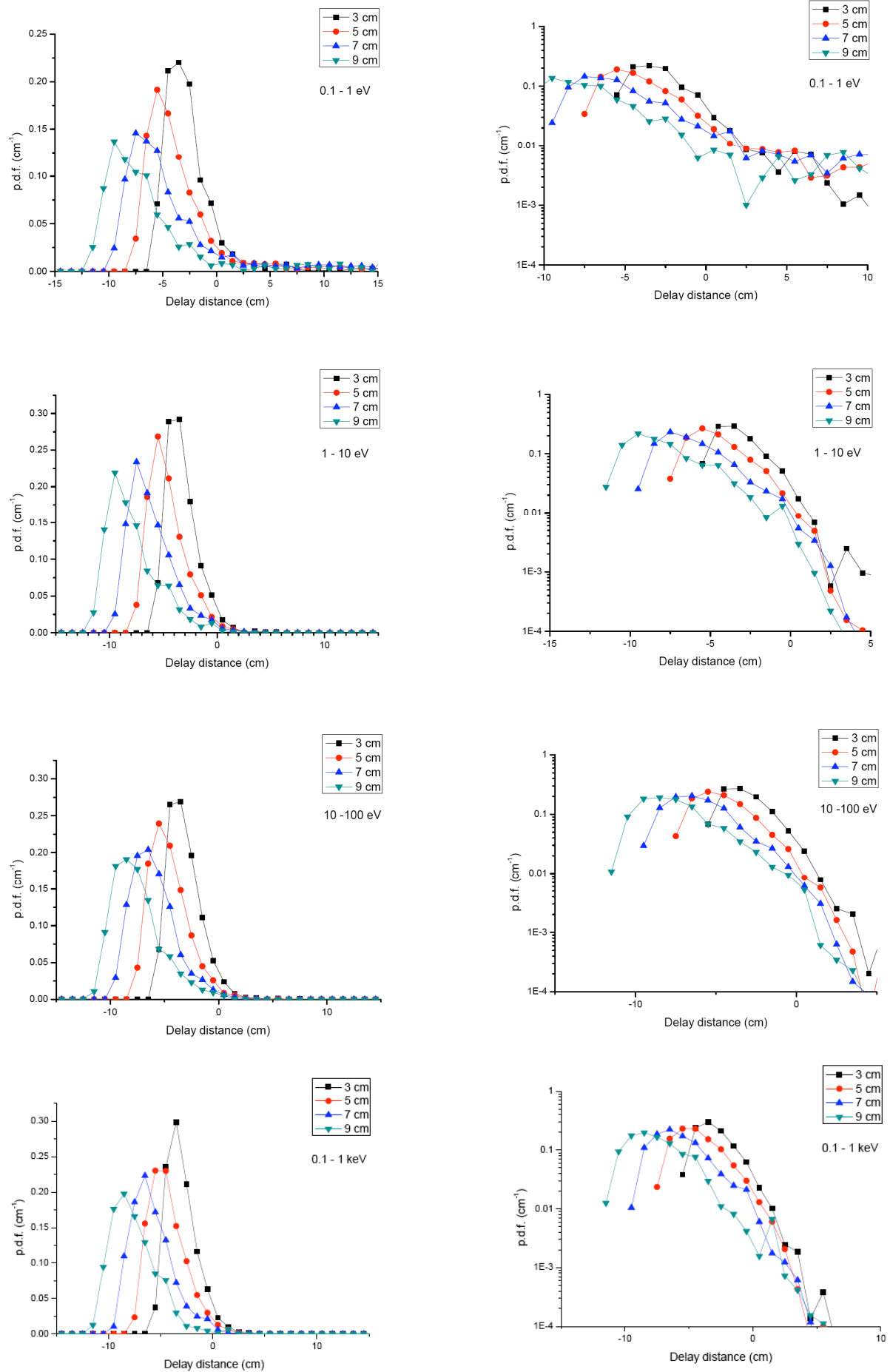


**Figure 21-a** Delay distance distributions (left linear, right logarithmic) for the R=2.5 cm target with various moderator thicknesses (no shielding); gaussian beam;  $0.1 \text{ eV} < E < 1 \text{ keV}$

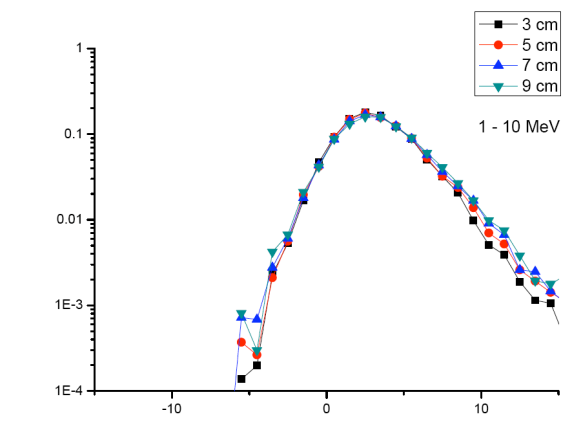
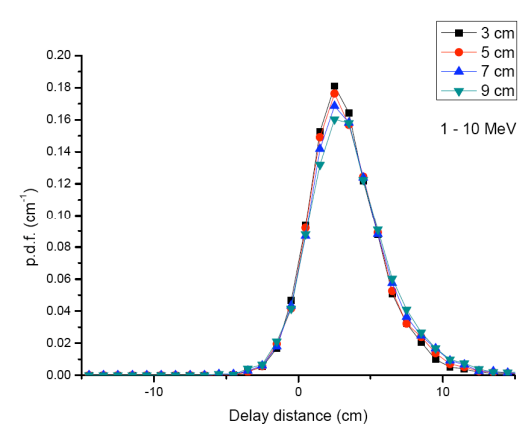
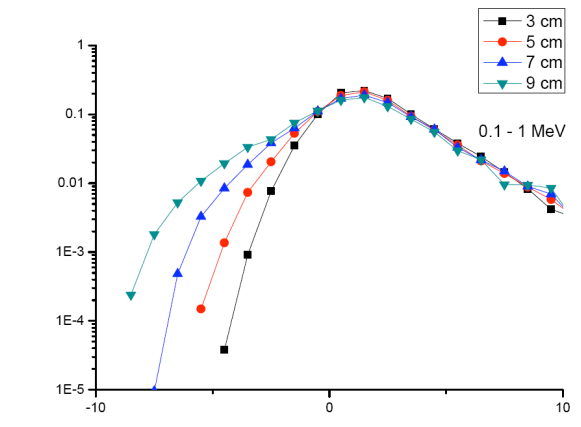
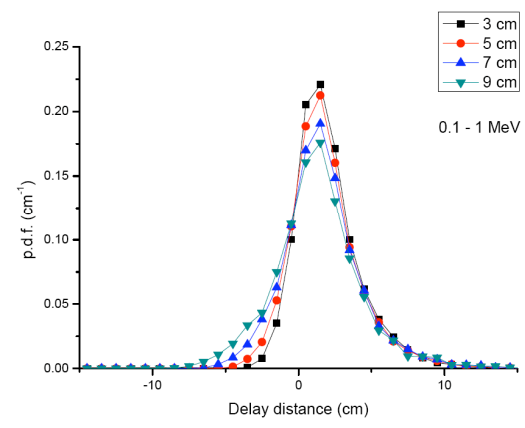
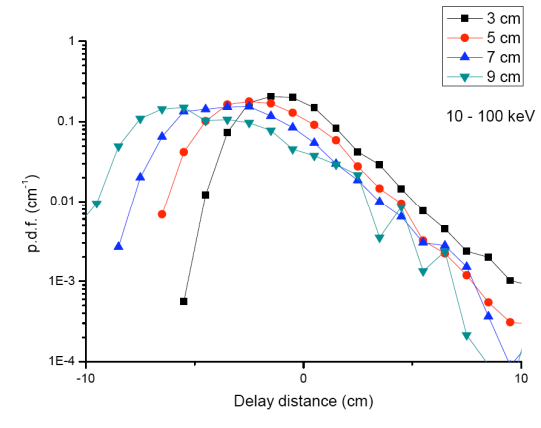
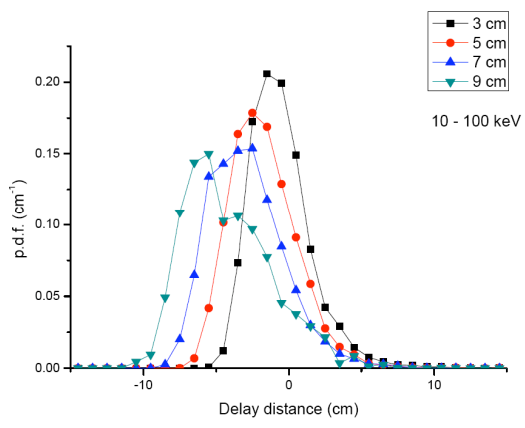
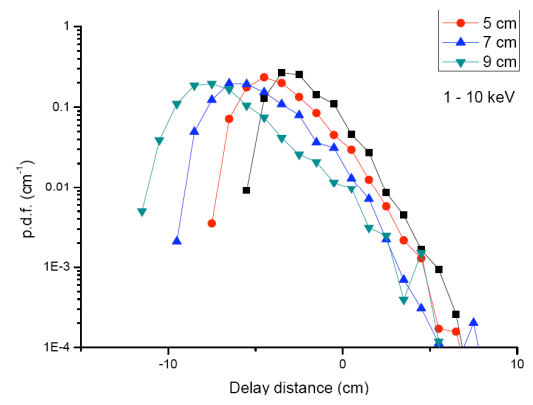
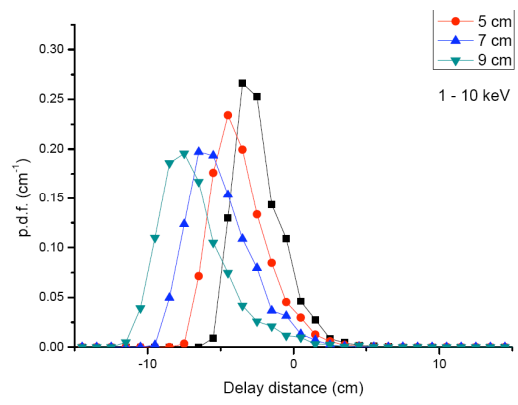


Figure 21-b Delay distance distributions for various moderator thickness;  $1 \text{ keV} < E < 10 \text{ MeV}$

## 4.6 TARGET SHIELDING AND BEAM DUMP

The integration of the neutron radiator inside the beam dump seems quite natural, owing to the required characteristics (fig. 11). The main problem here is the huge  $\gamma$ -flash coming from bremsstrahlung on the Ta target, what makes the use of heavy metal shielding almost mandatory. Then an adequate thickness of light hydrogenated material is necessary to moderate the big number of neutrons.

Several possibilities were investigated by means of the MCNP5 code and the dose profiles were calculated on the surface at 1 m distance from the target centre. The simulated structure has a quadratic, rather than cylindrical symmetry, for ease of construction. No high temperature materials, like graphite, were considered, owing to the modest level of deposited power. A summary of simulated configurations is shown in Table VI.

**Table VI: Side and rear dose profiles [Sv/e<sup>-</sup>] for neutrons and photons at 1 m from beam axis for several shielding materials (PE= Polyethylene)**

Materials	Side n [Sv/e <sup>-</sup> ]	Side $\gamma$ [Sv/e <sup>-</sup> ]	Total [Sv/e <sup>-</sup> ]	Rear n [Sv/e <sup>-</sup> ]	Rear $\gamma$ [Sv/e <sup>-</sup> ]	Total [Sv/e <sup>-</sup> ]
PE 55 cm thick, no Pb	1.19E-18	9.04E-17	9.16E-17	4.66E-18	4.02E-16	4.07E-16
Al 55 cm thick, no Pb	2.25E-17	2.56E-18	2.51E-17	2.93E-17	1.80E-17	4.73E-17
PE 55 + 30 Pb	2.02E-18	6.13E-22	2.02E-18	1.03E-17	2.61E-21	1.03E-17
55 PE + 0.2Cd + 15 Pb	2.99E-18	8.57E-20	3.07E-18	1.81E-17	5.24E-19	1.86E-17
55 PE+10borax+15Pb	2.38E-18	5.49E-20	2.43E-18	1.60E-17	3.67E-19	1.64E-17
20 Pb + 40 PE	8,08E-20	7,04E-19	7,85E-19	1,23E-19	8,31E-19	9,54E-19
20 Pb + 50 PE	4,31E-20	4,50E-19	4,93E-19	4,76E-20	5,22E-19	5,70E-19
Pb 20 + PE 50 + Pb 10	5.36E-20	2.59E-21	5.62E-20	5.59E-20	2.93E-21	5.88E-20

The first stage of the computations consisted in selection of the optimal thickness of the neutron shield. Aluminum, which had been adopted elsewhere [39], and Polyethylene were investigated. Thickness of both materials varied from 20 cm to 75 cm, with a 5 cm increment. Polyethylene is a better neutron moderator but aluminum reduces  $\gamma$ 's more efficiently. Nevertheless, because the gamma dose can be easily reduced by means of lead, it was decided to use Polyethylene as neutron shield and the optimal thickness of this material appeared to be 55 cm.

In the second step an external layer of lead was added. The range 10 cm up to 30 cm with an increment of 5 cm was examined. A 55 cm layer of Polyethylene followed by 30 cm of lead turned out to be the best configuration. The total dose in the foregoing arrangement originates actually from neutrons only. Hence, it is crucial to reduce the neutron component. Some attempts were carried out to get rid of thermal neutrons by means of cadmium or borax placed between Polyethylene and lead, however they failed. The next idea was to introduce the internal layer of lead since still some photons and electrons leave the target and may produce photoneutrons in the neutron shield.

The final series of the simulations consisted of three steps. First, a fixed layer of Polyethylene (40 cm was arbitrary selected) followed the internal lead shield of a varying thickness (5 cm to 25 cm with a 5 cm increment). The optimal size of the internal lead appeared to be 20 cm. Then the 20 cm layer of lead was followed by the neutron shield of the varying thickness (20 cm to 55 cm with a 5 cm increment). These calculations suggested the use of 50 cm of Polyethylene. Finally, the layers of 20 cm of lead and of 50 cm of Polyethylene were followed by the external layer of lead (5 cm, 10 cm and 15 cm were examined).

The optimum thicknesses of the beam dump appears to be 20 cm for the internal layer of lead, 50 cm of Polyethylene and 10 cm of external lead. The total dose is about two orders of magnitude

lesser than in the configuration with 55 cm of Polyethylene followed by 30 cm of external lead. Although the photon dose rises significantly the decrease of the neutron dose recompenses this effect with surplus.

The resolution function is not clearly affected, as shown in the fig. 22-a for pointlike beam, where the advantages of the small radius target are clearly not spoiled by the shielding, while above 10 keV is

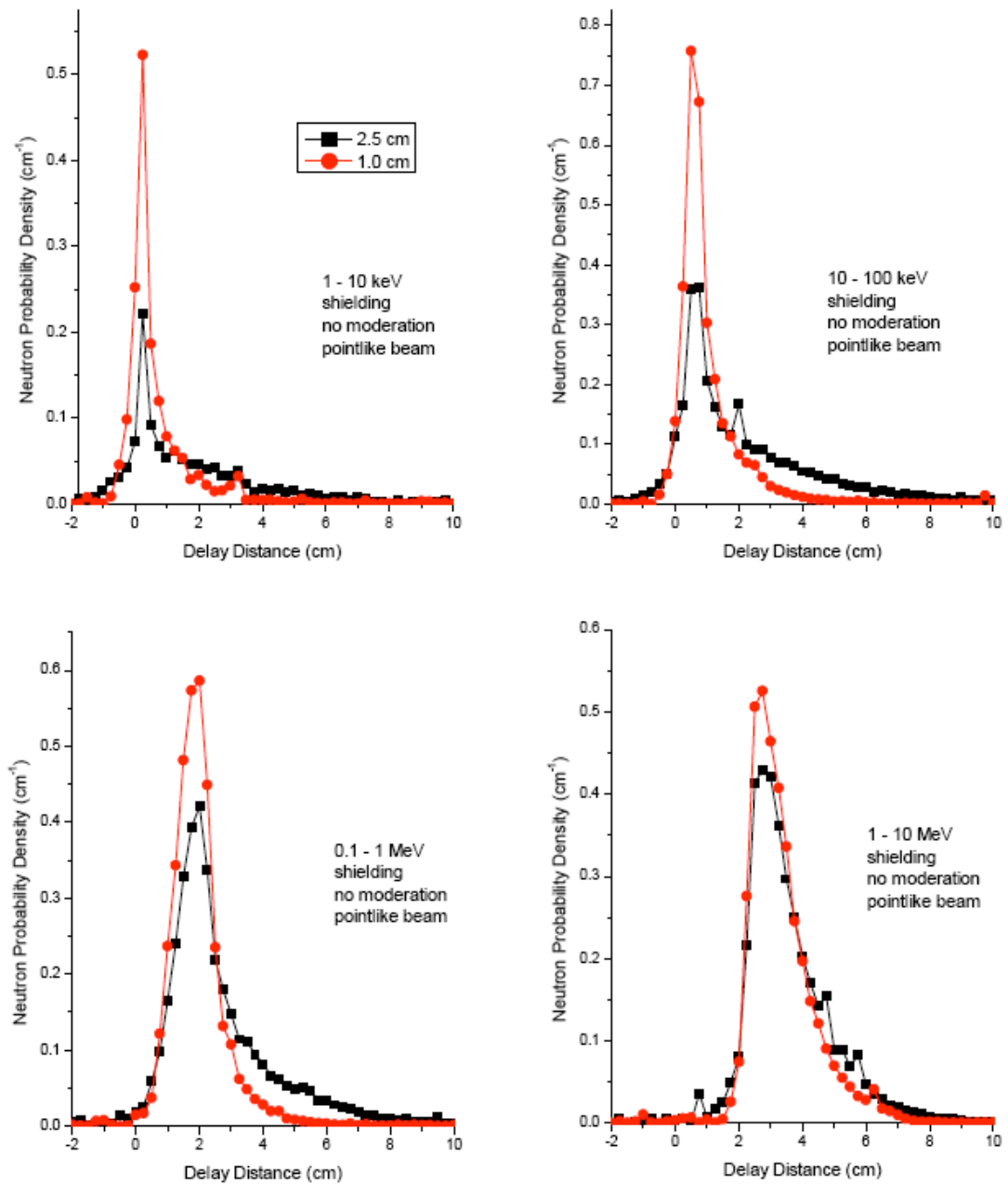


**Figure 22-a Delay-distance distributions of the shielded source for the pointlike beam**

the gaussian shape of the beam that affects the resolution (fig. 22-b)

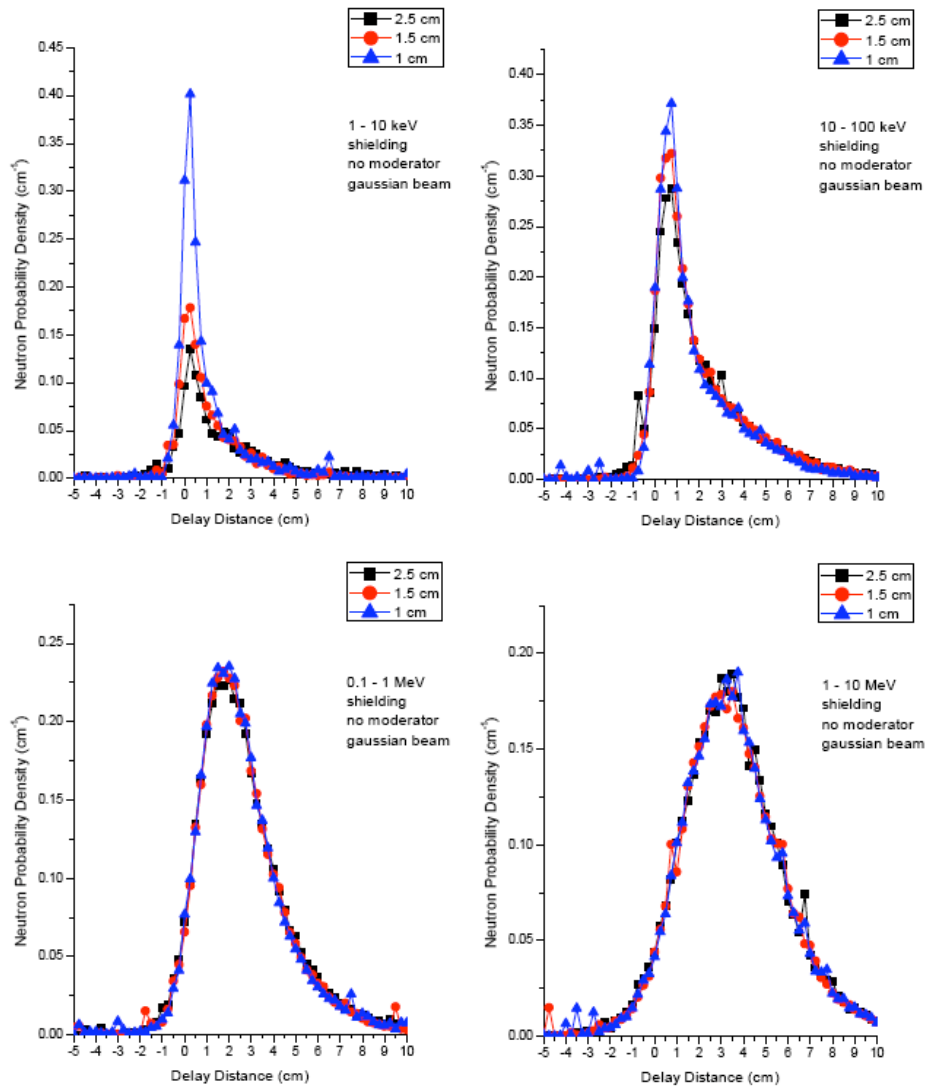


**Figure 22-b Delay-distance distributions of the shielded source for the gaussian beam**

The insertion of target into the shielding will not affect significantly the spectrum as it shown in the plots (fig. 23) for the 3 target radii with gaussian beam. The only effect is an increase of low energy background, due to scattered neutrons inside the target chamber.

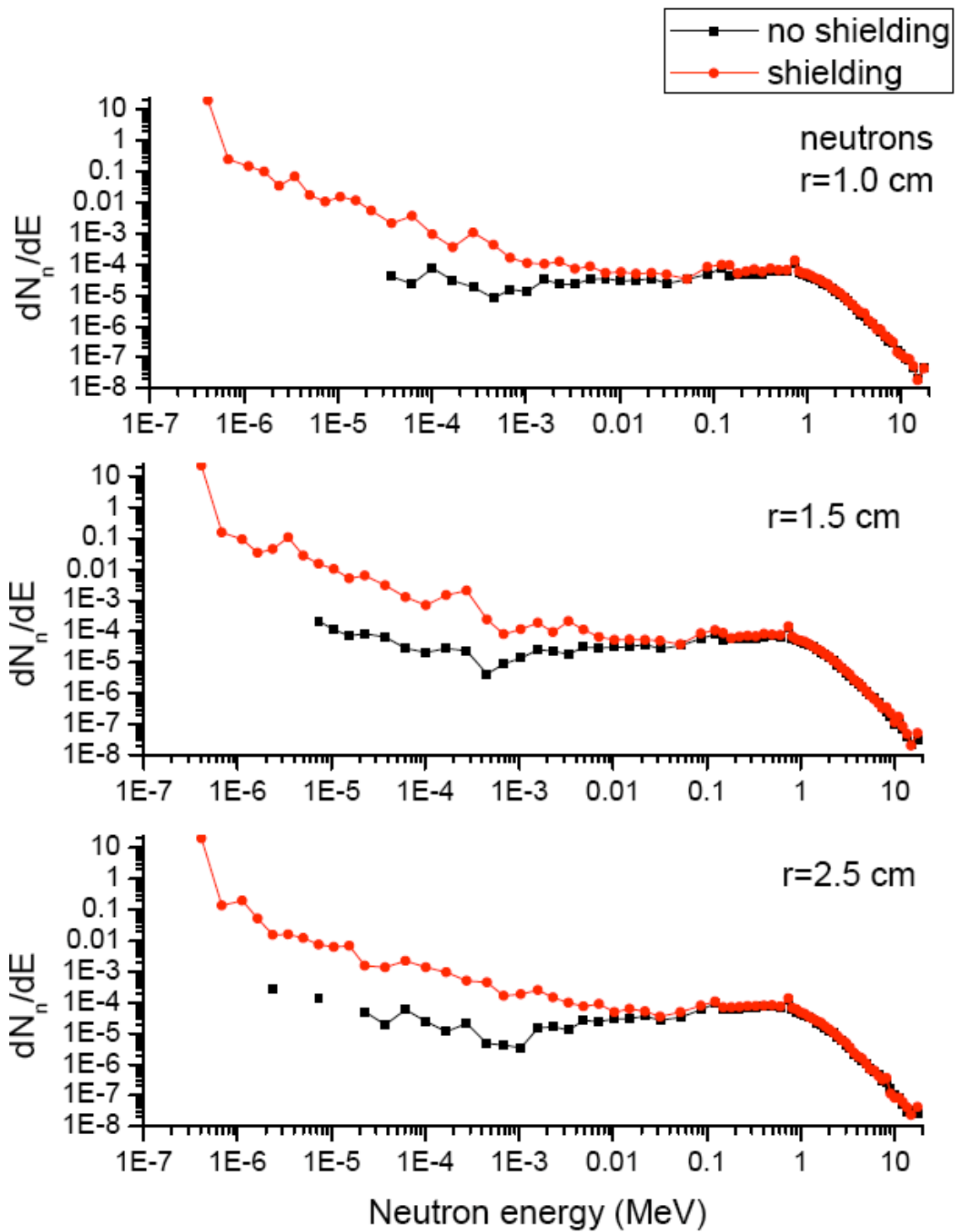


Figure 23 Effects on neutron spectrum of shielding structure for 3 target radii

## 4.7 NEUTRON BEAM COLLIMATORS

Purpose of collimators is to create a spatially well-defined beam, with a size appropriate for irradiation of samples. Also, a fundamental requirement of a good collimator is the minimization of background and so the preservation of an acceptable energy resolution and an useful flux. The wall of the neutron tube here consists of simple Polyethylene (PE) and Lead, which are materials that require a special attention: PE is an efficient moderator but it undergoes neutron capture ( $\sigma = 6.6 \cdot 10^6$  [b] /  $v$  [m/sec]) easily, with emission of a 2.223 MeV photon from the  $^1\text{H}(n,\gamma)^2\text{H}$  reaction. In the following figs. the delay-distance distributions for the uncollimated beam and for two simple collimator design are compared. The R=2.5 cm target is chosen, no moderator effects are included. Two collimator configurations are sketched in fig 24.

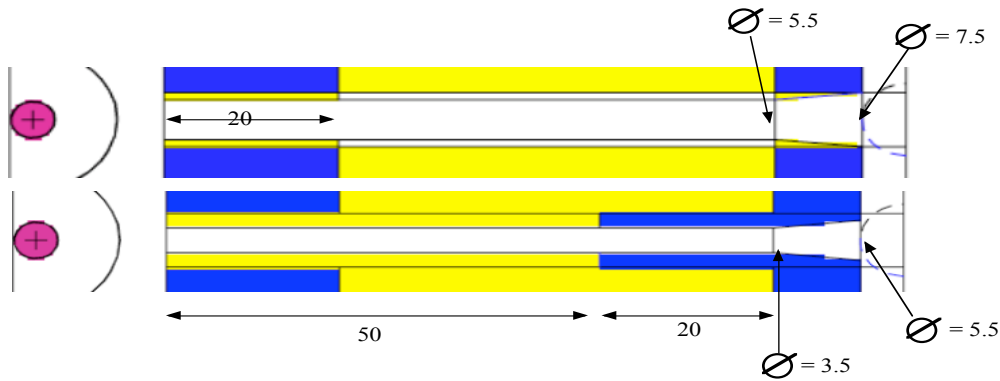


Figure 24 Collimators: 1 above, 2 below; (PE in yellow, Pb in blue, Ta in

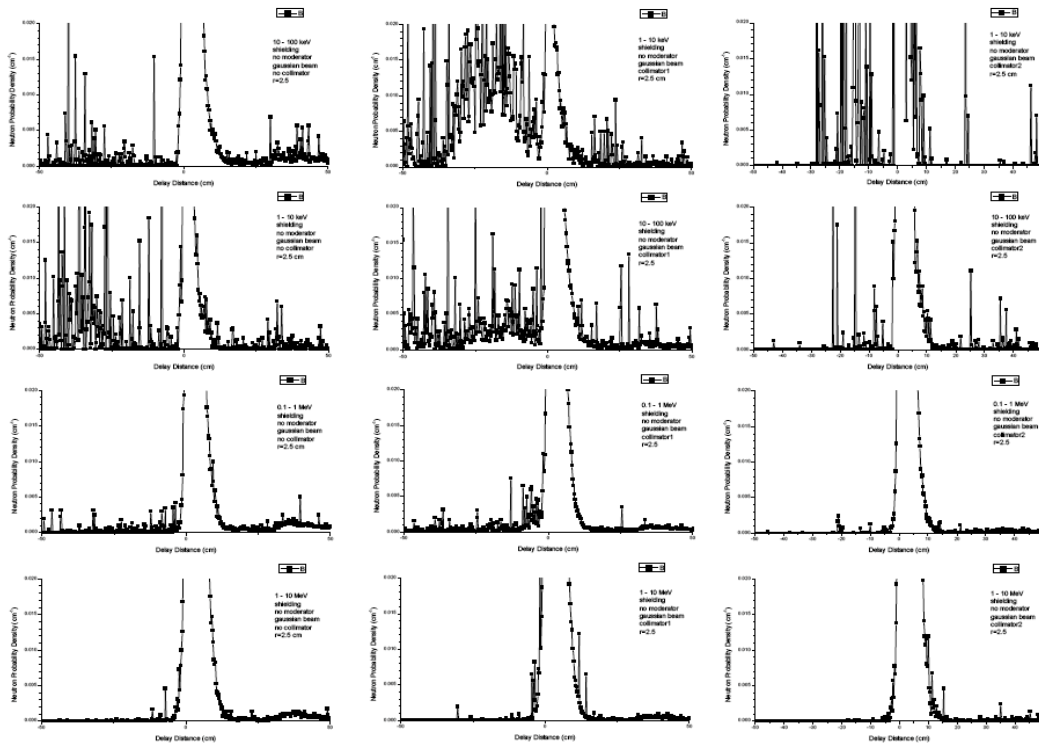
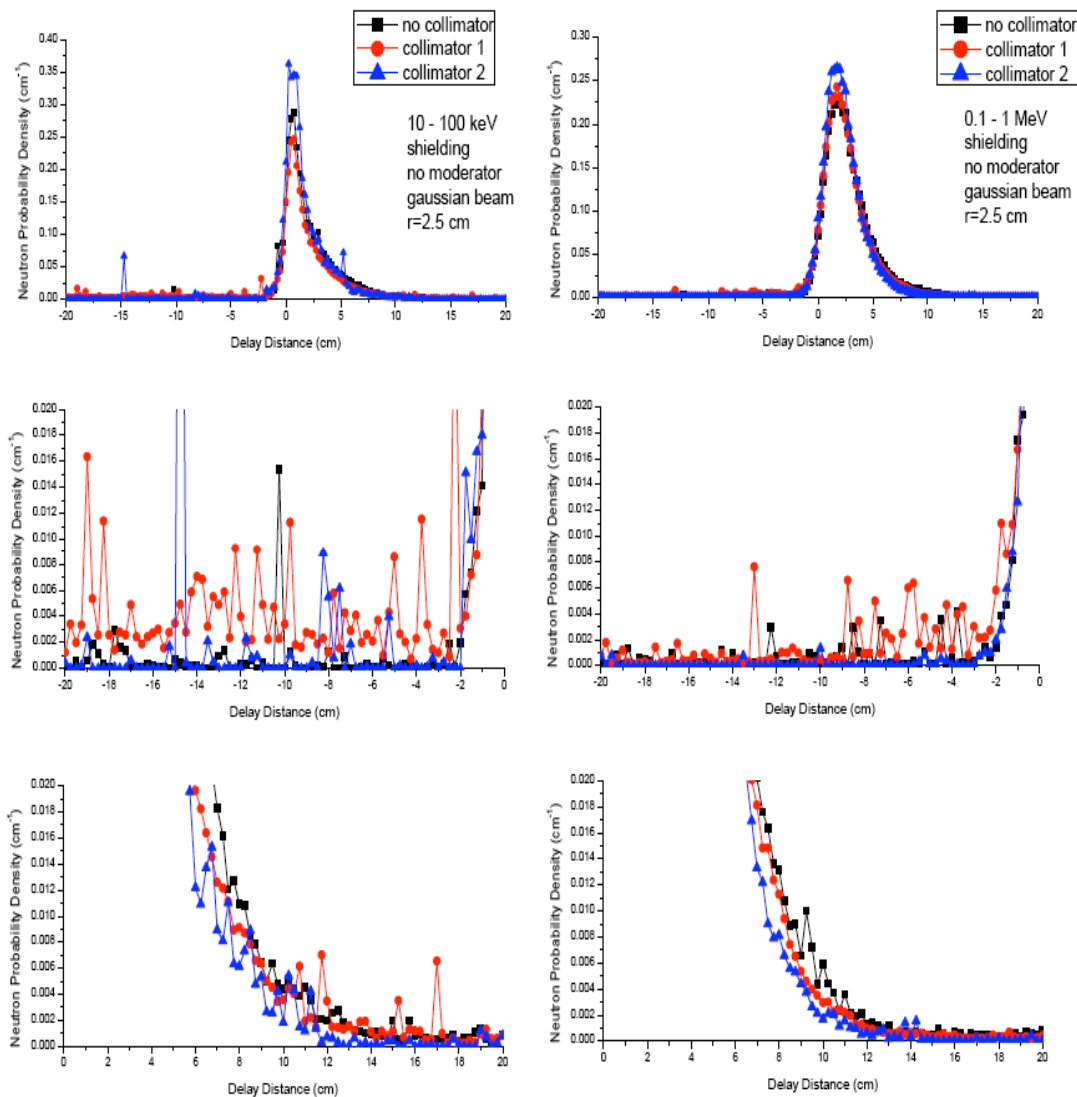


Figure 25 Noise reduction by comparing the uncollimated beam (left) with two collimators (1 middle, 2 right) for the R=2.5 cm target and gaussian beam (unmoderated spectrum)

In fig. 25 only the left and right 'tails' of the resolution function are shown for 4 energy intervals. The presence of out-of-peak particles, on both sides of it, is quite evident even in the higher-energy plots and seems enhanced by the action of collimator 1. The left side of the distributions is probably due to the presence of neutrons interacting along the PE walls or to  $\gamma$ -produced neutrons in the PE layers, while in case of collimators are due to higher energy neutrons which interact in the last PE structure (and they are more present in the low energy intervals, indeed). The right tail is mainly due to  $\gamma$ -produced neutrons in the PE layer and disappears by screening PE with the Pb, as in the collimator 2 structure. In fig 26 the three structures are compared together for energy intervals 10-100 keV and 100-1000 keV.

The practical effect of collimator 2 can be judged from fig. 27 where the radial profiles of photon and neutron flux at the collimator exit are shown.



**Figure 26 Comparison of RF in the 10 keV - 1 MeV range for un- and collimated beams**

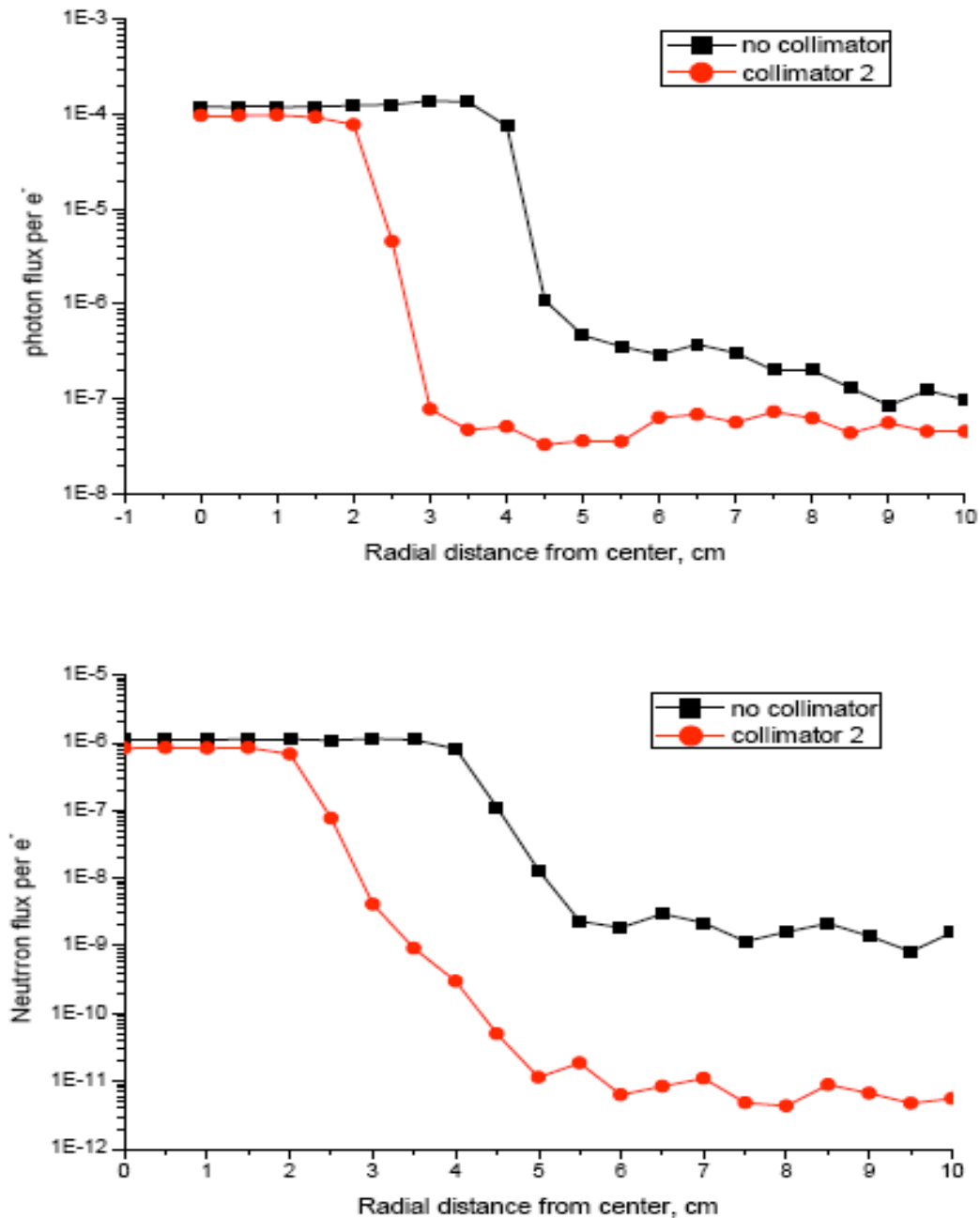


Figure 27 Un- and collimated radial profiles for  $\gamma$  (above) and n (below)

#### 4.8 RADIATION BACKGROUND AND NEUTRON PULSE STRUCTURE

Some preliminary estimate of the background particles,  $\gamma$ 's and electrons, at the detector position was already done for a 10  $X_0$  Tantalum target with radius 2.5 cm [45] at 1 GeV. No shielding was considered. The FLUKA results are reproduced in the following tables and show an average (solid-angle) neutron current of  $2.70 \cdot 10^{-6}$  against a photon current of  $4.46 \cdot 10^{-4}$  and electron current of  $8.58 \cdot 10^{-6}$  [ $1/\text{cm}^2/e^-$ ] at 1 m distance from the beam axis. The situation improves a bit when looking at the radiation field at  $90^\circ$ , where the neutron current is  $2.82 \cdot 10^{-6}$  vs.  $2.27 \cdot 10^{-4}$  and  $3.26 \cdot 10^{-6}$  respectively, but still there are almost 2 orders of magnitude more photons than neutrons!

In order to make a realistic estimate of the background level, calculations have been repeated with MCNP5 for the full geometry system and collimator n. 2 in place. Particle currents and their

spectra are shown in fig. 28. Owing to the quite complicated geometry, the statistics is somewhat poor, especially for electrons and positrons.

Although the  $\gamma$ -flash, which has a typical flytime of  $\sim 3$  ns, can be well separated from the

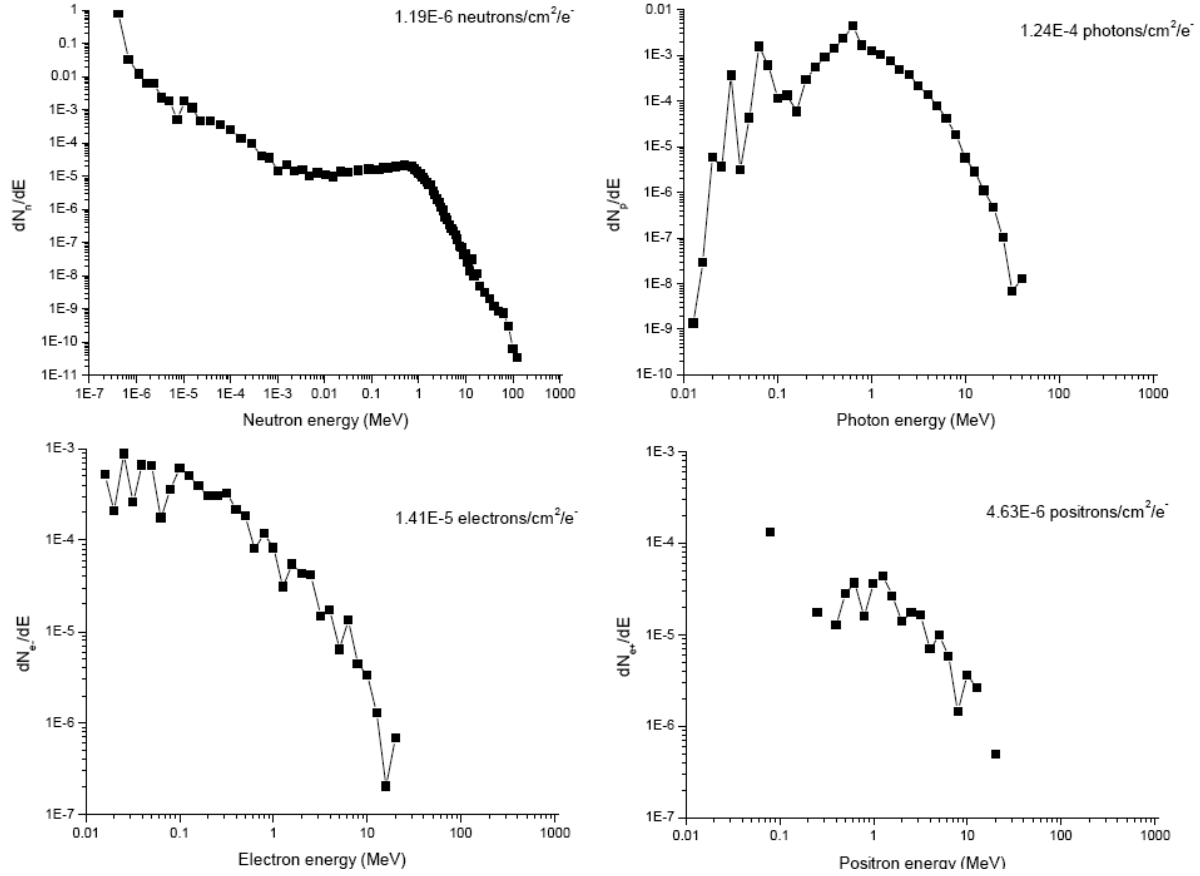


**Figure 28 The particle spectra at the exit of collimator 2 (full shielding, no moderator, gaussian beam)**

neutron pulse (1 MeV neutrons have a flytime of 72 ns) by using fast scintillators, it is not always possible to use these detectors for physics experiments. So some 'shadowing' system has to be considered, provided it doesn't spoil the neutron pulse spectrum.

The maximum usable neutron energy depends also on detector dead time, while the minimum depends on the primary beam repetition rate (LNF Linac + SPARX).

#### 4.9 ENERGY RESOLUTION AND FITTING FUNCTION

The relative energy resolution of a TOF facility is given by the well-known formula:

$$\frac{\delta E_n}{E_n} = 2 \left\{ \sqrt{\left[ \frac{\delta L}{L} \right]^2 + \left[ \frac{\delta t}{t} \right]^2} \right\}$$

which, when combined with the kinetic energy expression for a non-relativistic neutron, gives

$$\frac{\delta E_n}{E_n} = \frac{2}{L} \sqrt{\delta L^2 + \frac{2E_n}{M_n} \delta t^2}$$

where  $L$  is the length of the flightpath and  $E_n$  is the neutron energy at detection point. Here  $\delta L$  is a pure flightpath uncertainty, which includes neutron generation's point in the target (always assumed in its centre), scattering inside target and moderator and perhaps in the neutron transport channel up to the detector. The time uncertainty  $\delta t$  here includes the primary electron beam's pulse duration only, without detector's resolution, DAQ electronics etc.

Doppler effect contribution, due to thermal motion of target nuclei, is not considered here.

It is convenient and customary to evaluate the energy resolution of a TOF facility at a flightpath  $L$  as function of the *delay distance*  $d = t \cdot v_n - L$ , where  $t$  is the time interval between neutron generation and detection and  $v_n$  is the neutron speed at detection. This allows one to use wide energy bins for most materials, as it will be seen soon.

Assuming that a neutron undergoes  $n-1$  collisions before being observed in a virtual infinitely thin detector and that the segment  $l_i$  between the  $i-1$  and the  $i$  collision is traveled at velocity  $v_i$ , we have obviously

$$d = \sum_{i=1}^n \frac{l_i}{v_i} v_n - L$$

Less obviously, this quantity may be negative if  $v_n \ll v_i$  for the shortest part of the neutron path (or  $l_i \gg l_n$ ), as it can be shown easily for  $n=2$ , also taking into account that the neutron generation point can be anywhere in the target, while the distance  $L$  is taken from target centre, usually.

Also, we can define the average time a neutron keeps the same energy or speed  $v$ :  $\tau = 1/(\Sigma_s \cdot v)$ ,  $\Sigma_s = \sigma_s N_a \rho / A$  [ $\text{cm}^{-1}$ ] being the 'macroscopic scattering cross section' or 'cross section per unit volume' and  $v$  is the neutron velocity. Here  $N_a$  is Avogadro's number,  $\rho$  is material's density and  $A$  the molecular weight, so the quantity  $\lambda = 1/\Sigma_s$  [ $\text{cm}$ ] is the 'mean free path' of neutrons in a given material.

But if the cross-section  $\sigma_s$  is quite independent on energy on a wide energy range, also the dependence  $\lambda(E)$  is quite weak in that energy range and it is clearly more interesting to study the resolution in terms of travelled distance than in terms of elapsed time, which is proportional to  $1/\sqrt{E}$ .

According to Groenewold-Groendijk [47], the delay-time distribution of moderated neutrons of initial energy  $E_0$  for  $E > 1$  eV from a point source is:

$$W(E_0 \rightarrow E; t) dE = \begin{cases} 0 & \text{for } t < 0 \\ \approx \frac{1}{E} e^{-\frac{t}{\tau(E)}} \frac{1}{2} \frac{t^2}{\tau(E)^2} dE & \text{for } t > 0 \end{cases} \quad [1]$$

The above eqn. gives the average number of slow neutrons within the energy interval  $[E, E+dE]$  at a time  $t$  after their start (which has to be weighted with the pulse time amplitude of the primary beam) and  $\tau(E) = \lambda(E)/\sqrt{E}$  is the average time a neutron keeps the energy  $E$  where  $\lambda(E)\sqrt{(2/M_n)}$  is the 'mean free path' of a neutron with energy  $E$  in a given material, as shown before.

Now it happens that the dependence  $\lambda(E)$  is quite weak in the range  $1-10^4$  eV (see table I in [47]), growing significantly only above 100 keV (the energy dependence of cross section in the unresolved resonance region of homogeneous materials is very weak indeed). But the high energy neutrons

contribute slightly to time dependence, as they are run through in a very short time. This justifies the assumption  $\lambda(E) = \text{const} = \lambda(1 \text{ eV})$  for the whole range.

So if we look at the above probability density function (p.d.f.), which is the product of the probability  $1/E \cdot dE$  of a neutron arriving in the interval  $[E, E+dE]$  irrespective of the number of collisions, and the probability of finding it at a time  $t$  after start, we have that at a given energy  $E_n$ :

$$f(t) = \frac{t^2}{2\tau_n^3} e^{-\frac{t}{\tau_n}}$$

This is a normalized,  $\chi^2$ -like distribution, with a mean of  $3\tau_n$ , a variance of  $3\tau_n$  and a FWHM of  $\Delta\tau = 2\sqrt{3}\tau_n \approx 1.85\sqrt{E_n}$  [us, eV] (see e.g. [47]).

By expressing the (1) formula with the variable change  $t/\tau_n = x/(\lambda(E)\sqrt{2/M_n}) = x/\Lambda(E)$  we get

$$W(E \rightarrow E_n; x) \approx \frac{1}{E_n \Lambda_n} \left(\frac{x}{\Lambda_n}\right)^2 \exp(-x/\Lambda_n)$$

where we introduce an equivalent distance  $x = (t/\tau_n) \cdot \Lambda_n = t \cdot \sqrt{2E_n/M_n} = t \cdot v_n$

Here the FWHM is  $2\sqrt{3}\Lambda = 2\sqrt{3} \lambda \cdot \sqrt{2/M_n}$  almost energy independent in a wide range, as we have seen.

So, although the special behaviour of the Resolution Function (R.F.) will be mainly dependent on target's material and geometry, but also on the observation angle, we can expect some features to be common to all cases in the direct spectrum, i.e.:

- a presence of  $d < 0$  values at low energy  $\sim 10 \text{ keV}$ , which increases up to  $\sim 0.1 \text{ MeV}$  and decreases again from  $\sim 1 \text{ MeV}$
- in the same region, a sharp enhancement of the  $d=0$  peak starting from  $\sim 30 \text{ keV}$ , which broadens again above  $1 \text{ MeV}$ . This is the region where neutron interactions have a low cross section.
- at high energy the R.F. is dominated by the beam pulse width and the varying birth locations of the neutrons.

The situation is quite different for the moderated spectrum, where the p.d.f. is significant at negative delay distances, even for thin moderators. This is caused by fast neutrons that undergo their final scattering close to the surface that is nearest to the detector.

The R.F. has a strong dependence on the thickness and shape of moderator, while it is less target-influenced especially at low energy, 1-10 eV. The optimization of the moderator must consider not only the maximum achievable flux, i.e. the moderator efficiency, but also the required resolution.

The R.F. distributions which are shown in figs. 21a-b represent just a preliminary approach to this optimization process.

#### 4.10 MECHANICAL DESIGN

A sketch of the mechanical structure of the neutron source in its various parts is shown in fig. 29. The terminal vacuum pipe from the accelerator is inserted into a shielding Pb end cap. To separate the high vacuum of the electron beam-line ( $\sim 10^{-9}$  mbar) from the neutron radiator zone (max pressure 1 mbar) probably a Beryllium window has to be used. Accurate calculations will be necessary, depending also on the effective beam power. A containing vessel, which is made of stainless steel, is necessary but is not shown in the picture. The weight of the totale structure will be probably around 20 tons, quite tolerable for installation on guiding rails.

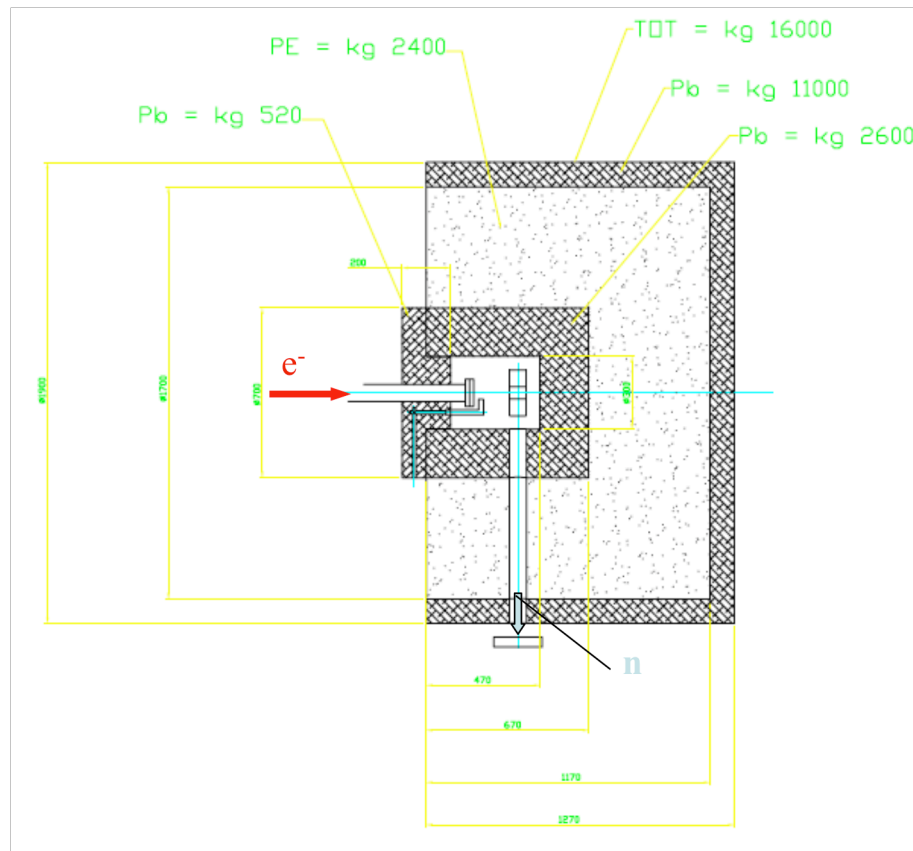


**Figure 29 Top view of the source with relevant dimensions and weights (in green); red arrow-electron beam, light blue arrow-neutron beam**

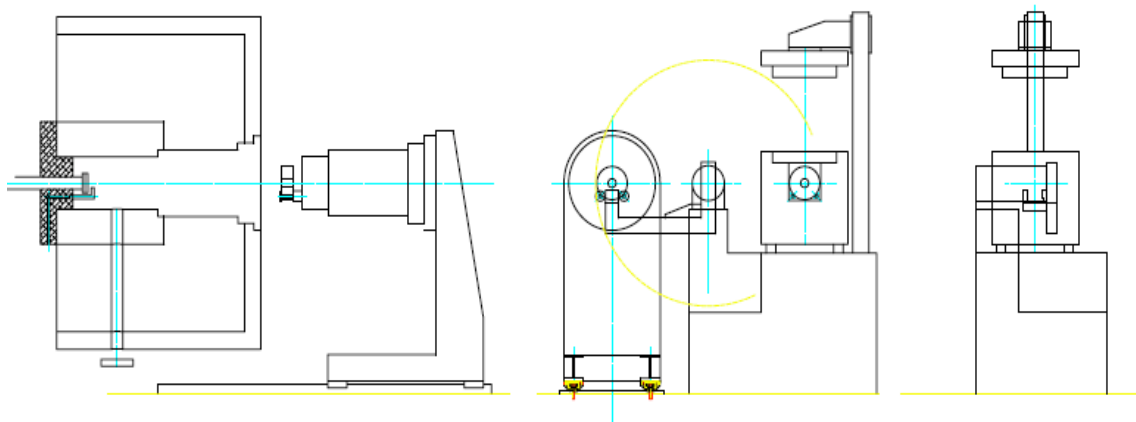


**Figure 30 The supporting mechanical structure**

A sketch of the supporting structure is shown in fig. 30 in its basic features. The rear part of the shielding is removable and acts also as support of the target/moderator system in the operating position; the supporting framework is sliding on guides. The radiator removal system and the safe repository for the irradiated components are also shown.

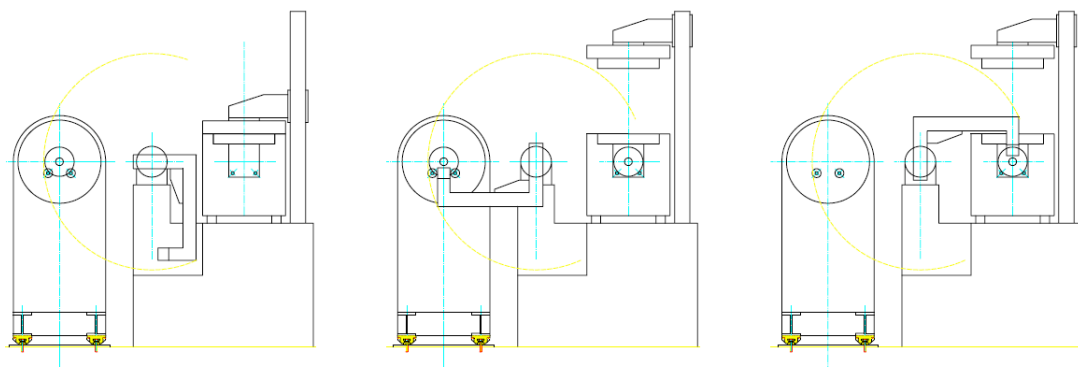


**Figure 31 The neutron radiator handling system**

The neutron radiator handling system is illustrated more clearly in fig. 31. A mechanical arm is used to decouple the radiator system from the beam dump/rear shielding structure and drop it into the repository during the non-operating periods of the facility. The system is fully remote-controlled and redundant to meet radiation safety requirements.

## 5. Personnel and cost estimate

The project duration is estimated in 24 months, according to the following table, which describes also the required personnel units:

**Table VII : Time schedule and personnel resources**

Personnel/Months from approval	6	6	6	6
An expert physicist 1	Define Eng. Project with contractor	Apparatus Construction Survey	Apparatus Installation&integration	Commissioning of the facility
An expert physicist 2	Collimator and background simulations	Completion of simulation work	Preparation for exp. determinations. of beam characteristics(flux, RF, beam profile, background)	Commissioning of the facility
A post-doc starting physicist	Beam Monitors design	Ext. Beam test on detectors and calibration	Preparation for exp. determinations. of beam characteristics	Commissioning of the facility
A mechanical technician		Apparatus Construction Survey	Apparatus Installation&integration	
A skilled electronic technician	Assistance on Beam Monitor design	Assistance on Ext. Beam test	Development of fast electronics for exp. determination of beam characteristics	Commissioning of the facility

A very preliminary and conservative estimate of materials and service costs gives following results:

- Lead Shieldings: 120 k€
- Target, moderator and water recirculation system: 10 k€
- Polyethylene shielding: 2 k€
- Stainless steel external container: 10 k€
- Mechanical Support of the rear part of beam dump, removing system, whole security, command and control system: 40 k€

Detectors and associated electronics:

- Beam monitor, made of Li thin foils with an array of silicon detectors observing the  ${}^6\text{Li}(n,\alpha)\text{T}$  reaction, and 4 channels of Flash ADC readout: 50 k€

- Beam monitor to determine the neutron flux over a wide energy range: 2 fission chambers, like the PTB ones, cost 20 k€ each, with 4 channels Flash ADC each for DAQ, at ~ 7 k€/channel for a whole cost of = 40 + 8•7 ~ 100 k€.
- Two fast BaF<sub>2</sub> scintillators for neutron capture measurements: 16 k€ each, 32 k€ totally.

Total cost of material and services: 354 k€

## 6. Conclusions

A general presentation of the scientific case for a neutron time-of-flight facility in the Rome Research Area is given and its main features are discussed. There is a growing interest in nuclear data worldwide and the existing neutron sources are clearly insufficient. Also the possibility of doing fundamental and neutron physics research seems appealing.

The possibility of a flux of  $10^5$  n/cm<sup>2</sup>/sec with 2-3% energy resolution for neutron energies below 1 keV seems within reach, despite the low power of the primary beam presently available and given the difficult experimental conditions. Since the true figure-of-merit of such facilities is maximum flux per unit energy resolution, the optimization criteria for the main parts of the neutron source, target, moderator, radiation shielding, collimators etc. are based on extensive simulations and studies of the delay distance distributions, according to the most common practice in the field. A best fit study of the resolution function is still in progress, to be used in evaluation codes like SAMMY[48], together with the optimization of the neutron collimator and detector.

## Acknowledgments

We thank Dr. Sergio Bertolucci, ex-LNF Director, for his support at the beginning of this project and Prof. Mario Calvetti, LNF Director in charge, for his constant encouragement and financial support during the stay of Dr. V. Angelov at LNF.

This work was partially supported by the European Commission under TARI Contract No RII3-CT 2004-506078.

## References

- [1] <http://www.nea.fr/html/dbdata/hprl/>
- [2] F.J. Hambsch et al., "The standard branching ratio  $^{10}\text{B}(n,\alpha_0)$  to  $^{10}\text{B}(n,\alpha_1)$ ", *Journal of Nucl. Sci. and Techn.*, Suppl. 2, 1402-1405(2002).
- [3] <http://www.efnudat.eu>
- [4] <http://t2.lanl.gov/njoy/>
- [5] F. Corvi et al., "Neutron Data Measurements for Waste Transmutation at GELINA", *Journal of Nucl. Sci. and Techn.*, Suppl. 2, 1067-1072(2002).

- [6] "Accelerator and Spallation Target Technologies for ADS Applications", NEA Report No. 5421, OECD 2005.
- [7] <http://www.sckcen.be/myrrha>
- [8] <http://nuklear-server.fzk.de/eurotrans/>
- [9] G. Aliberti et al., "Impact of Nuclear Data Uncertainties on Transmutation of Actinides in Accelerator-Driven Assemblies," *Nucl. Sci. Eng.*, **46**, 13-50 (2004)
- [10] G. Aliberti et al., "New Covariance Data and Their Impact on ADS Designs" in Proc. of AccApp Conference, Pocatello, ID, USA, (July-August 2007).
- [11] Generation IV International Forum (GIF), Annual report 2008.
- [12] "Nuclear Data Needs for Generation IV Nuclear Energy Systems," April 14-25, 2003, BNL, 2003.
- [13] R.A. Forrest, "Importance diagrams-a novel presentation of the response of a material to neutron irradiation", *Fusion Engineering and Design* **43** (1998) 209-235.
- [14] R.A. Forrest, "The activation system EASY-2007", *Journal of Nuclear Materials* **386-388** (2009), p. 878-881.
- [15] P. E. Koehler et al., "Resonance analysis of  $^{147}\text{Sm}(n,\alpha)$  cross sections: Comparison to optical model calculations and indications of nonstatistical effects", *Phys. Rev. C* **69**, 015803 (2004).
- [16] D.K. Galloway et al., "Periodic Thermonuclear X-Ray Bursts from GS 1826–24 and the Fuel Composition as a Function of Accretion Rate", *Astrophys. J.* **601**, 466 (2004).
- [17] S.E. Woosley et al., "Models for Type I X-Ray Bursts with Improved Nuclear Physics", *Astrophys. J. Suppl.* **151**, 75 (2004).
- [18] R.S. Stone, "Neutron therapy and specific ionization", *Am. J. Roentgenol.*, **59**:771-784, 1948.
- [19] W.H. Sweet, "The use of nuclear disintegrations in the diagnosis and treatment of brain tumor", *N. Engl. J. Med.*, **245**:875-878, 1951.
- [20] F.M. Waterman et al., "The use of  $^{10}\text{B}$  to enhance the tumour dose in fast neutron therapy", *Phys. Med. Biol.* **23**(4):592-602, 1978.
- [21] C. van Vliet-Vroegindeweyj et al., "Microdosimetry Model for Boron Neutron Capture Therapy: Determination of Microscopic Quantities of Heavy Particles on a Cellular Scale", *Radiation Research*, **155**, No. 3 (March 2001), pp. 490-497.
- [22] ICRU Report 48, "Phantoms and Computational Models in Therapy", New York, 1992.
- [23] A.M. Lane, R.G. Thomas, "R-Matrix Theory of Nuclear Reactions", *Rev. Mod. Phys.* **30**, 1958, 257-353.
- [24] T. Guhr et al., "Random-matrix theories in quantum physics: common concepts", *Phys. Rep.* **299**, 189 (1998).
- [25] J.M. Pearson et al., "Nuclear mass formulas for astrophysics", *Nucl. Phys. A* **777**, 623 (2006).
- [26] H. Goutte et al., "Mass and kinetic energy distributions of fission fragments using the Time Dependent Generator Coordinate Method", *Phys. Rev. C* **71**, 024316 (2005)
- [27] E. Monahan, et al., "Relation Between Fine and Intermediate Structure in the Scattering of Neutrons by Fe", *Phys. Rev. Lett.*, **20**, 1119 (1968)
- [28] J.S. Nico and W. M. Snow, "Fundamental Neutron Physics", *Ann. Rev. Nucl. Part. Sci.* **55** (2005), p. 27-69.
- [29] A. Frank et al., "Probing additional dimensions in the universe with neutron experiments", *Physics Letters B* **582** (2004) 15–20.
- [30] G. N. Kim et al., "Measurement of photoneutron spectrum at Pohang Neutron Facility", *Nucl. Instr. and Meth. in Phys. Res. A* **485** (2002) 458.
- [31] K.H. Guber et al., "Neutron cross-section measurements at ORELA", Proc. of ORELA Workshop, July 14-1, 2005.
- [32] P.E. Koehler, "Comparison of white neutron sources for nuclear astrophysics experiments using very small samples", *Nucl. Instr. and Meth. in Phys. Res. A* **460** (2001) 352.
- [33] C. Coceva et al., "On the figure of merit in neutron time-of-flight measurements", *Nucl. Instr. and Meth. in Phys. Res. A* **489** (2002) 346.

- [34] D. Alesini et al., "Conceptual design of a high-brightness linac for soft X-ray SASE-FEL source", *Nucl. Instr. and Meth. in Phys. Res. A* **507** (2003) 502.
- [35] D. Alesini et al., "The SPARC project: a high-brightness electron beam source at LNF to drive a SASE-FEL experiment", *Nucl. Instr. and Meth. in Phys. Res. A* **507** (2003) 345–349.
- [36] SPARX Proposal, <http://www.frascati.enea.it/SPARX/sparx.pdf>
- [37] S. Bartalucci et al., "Conceptual design of an intense neutron source for time-of-flight measurements", *Nucl. Instr. and Meth. in Phys. Res. A* **575** (2007) 287-291.
- [38] E. Altstadt et al., "A photo-neutron source for time-of-flight measurements at the radiation source ELBE", *Ann. Nucl. En.* **34** (2007) 36-50.
- [39] M.J. Berger et al., "Bremsstrahlung and Photoneutron from thick Tungsten and Tantalum targets", *Phys. Rev. C* **2** (1970) 621-631.
- [40] C. W. Fabjan et al., "Calorimetry in High-Energy Physics", *Ann.Rev.Nucl.Part.Sci.* **32** (1982) 335.
- [41] X-5 Monte Carlo Team, "MCNP A general Monte Carlo N-Particle Transport Code, Version 5", LA-UR-05-8617
- [42] W. P. Swanson, "Radiological Safety Aspects of the operation of Electron Linear Accelerators, IAEA Technical Reports Series No. 188 (1979).
- [43] N. Watanabe, "Neutronics of pulsed spallation neutron sources", *Rep. Prog. Phys.* **66** (2003) 339-381.
- [44] M. Flaska, "A compact fast-neutron producing target for high resolution cross section measurements", PhD Thesis, IOS Press (2006).
- [45] S. Bartalucci et al., "Preliminary study of a target-moderator assembly for a linac-based neutron source", IFJ Kraków Report No. 1961/PN (2005).
- [46] H.J. Groenewold et al., "Non-thermal neutron cascade", *Physica XIII*, (1947) 141-152.
- [47] C. Coceva et al., "Calculation of the ORELA neutron moderator spectrum and resolution function", *Nucl. Instr. and Meth.*, **211** (1983) 459-467.
- [48] "Updated user's guide for Sammy", October 2008, ORNL/TM-9179/R8.